AMERICAN SOCIETY FOR MICROBIOLOGY | Molecular and Cellular Biology®

RESEARCH ARTICLE

The N-Terminal Tail of Histone H3 Regulates Copper Homeostasis in *Saccharomyces cerevisiae*

Sakshi Singh,[a] Rakesh Kumar Sahu,[a] Raghuvir Singh Tomar[a]

[a]Laboratory of Chromatin Biology, Department of Biological Sciences, Indian Institute of Science Education and Research Bhopal, Bhopal, India

Sakshi Singh and Rakesh Kumar Sahu contributed equally to this work. Author order was determined by the fact that Sakshi Singh initiated and performed more experiments and Rakesh Kumar Sahu did more experimental designing, result analysis, and figure preparation.

ABSTRACT Copper homeostasis is crucial for various cellular processes. The balance between nutritional and toxic copper levels is maintained through the regulation of its uptake, distribution, and detoxification via antagonistic actions of two transcription factors, Ace1 and Mac1. Ace1 responds to toxic copper levels by transcriptionally regulating detoxification genes *CUP1* and *CRS5*. Cup1 metallothionein confers protection against toxic copper levels. *CUP1* gene regulation is a multifactorial event requiring Ace1, TATA-binding protein (TBP), chromatin remodeler, acetyltransferase (Spt10), and histones. However, the role of histone H3 residues has not been fully elucidated. To investigate the role of the H3 tail in *CUP1* transcriptional regulation, we screened the library of histone mutants in copper stress. We identified mutations in H3 (K23Q, K27R, K36Q, Δ5-16, Δ13-16, Δ13-28, Δ25-28, Δ28-31, and Δ29-32) that reduce *CUP1* expression. We detected reduced Ace1 occupancy across the *CUP1* promoter in K23Q, K36Q, Δ5-16, Δ13-28, Δ25-28, and Δ28-31 mutations correlating with the reduced *CUP1* transcription. The majority of these mutations affect TBP occupancy at the *CUP1* promoter, augmenting the *CUP1* transcription defect. Additionally, some mutants displayed cytosolic protein aggregation upon copper stress. Altogether, our data establish previously unidentified residues of the H3 N-terminal tail and their modifications in *CUP1* regulation.

KEYWORDS copper, metal homeostasis, Cup1 metallothionein, histone modification, Ace1, transcription regulation, protein aggregation, epigenetics, histones, copper response, yeast

Copper is an essential micronutrient but also acts as a double-edged sword. Copper concentration inside the cell needs to be maintained by copper homeostatic mechanisms. Its uptake and detoxification mechanisms operate inside the cell to control copper starvation and toxicity. Different mechanisms such as influx, delivery machinery (i.e., chaperones), efflux, and copper chelation by metallothioneins (MTs) are coordinated effectively to keep this delicate balance in check (1). Copper metal functions as a cofactor, required by the enzymes involved in different biological processes such as detoxification of superoxides (SOD1) (2), regulation of iron homeostasis (Fet3) (3), and mitochondrial respiration (cytochrome *c* oxidase) (4). The copper uptake system involves copper transporter Ctr1, Ctr3, and Cu/Fe reductases which are present on the cell membrane (5), and the copper detoxification system consists of copper metallothioneins Cup1, Crs5, and the superoxide scavenger enzyme SOD1 (6, 7). The genes for uptake and detoxification of copper are transcriptionally regulated under copper starvation and excess conditions to maintain its optimum level inside the cellular milieu. The transcription of uptake and detoxification genes is mediated by antagonistic actions of two transcription factors, namely, Mac1 (metal-binding activator) (8) and

Citation Singh S, Sahu RK, Tomar RS. 2021. The N-terminal tail of histone H3 regulates copper homeostasis in *Saccharomyces cerevisiae*. Mol Cell Biol 41:e00210-20. https://doi.org/10.1128/MCB.00210-20.

Address correspondence to Raghuvir Singh Tomar, rst@iiserb.ac.in.

Received 19 May 2020
Returned for modification 23 June 2020
Accepted 22 November 2020
Accepted manuscript posted online 30 November 2020
Published 25 January 2021

Ace1 (activator of *CUP1*) (9, 10). Mac1 acts as a nutritional copper sensor; it responds to low levels of copper and activates the expression of copper uptake genes such as transporter genes *CTR1*, *CTR3*, and *FRE1* (11, 12). Regulation of the copper uptake system occurs at both transcriptional and posttranscriptional levels via degradation of Ctr1 (13, 14). Mac1 contains a cysteine-rich motif in the transactivation domain, which binds to Cu^{1+} ions and performs its function (8). Ace1 acts as a toxic copper sensor, responding to elevated copper levels, and therefore activates expression of genes involved in copper detoxification such as *CUP1*, *SOD1*, and *CRS5*. Ace1 contains a copper regulatory domain which binds to copper via formation of tetra-copper thiolate clusters, which in turn lead to the formation of an active form of Ace1 (15). Activated Ace1 binds to the CUREs/*cis* elements (TX3/GCTG) present in the target gene promoters, activating their expression. Cup1 is the major metallothionein present in yeast cells, encoded by *CUP1*, whereas Crs5 MT has only a minor role in copper sequestration (12). Shuttling of copper from one organelle to another is mediated by copper chaperones such as Atx1 (Cu chaperone for Ccc2p present on the *trans*-Golgi network), Ccs1 (Cu chaperone for enzyme SOD1), and Cox17 (chaperone for mitochondrial enzyme cytochrome *c* oxidase [CCO]) (7).

The copper homeostasis in yeast is similar to that in mammalian cells, as the key factors involved in copper transport (Ctr1 and Ctr2), chaperones involved in copper delivery (Atx1, Ccs1, and Cox17), and copper-binding proteins (SOD1 and CCO) are conserved (1). Defects in copper metabolism have been associated with several human diseases such as Menke's disease, Wilson's disease, amyotrophic lateral sclerosis (ALS), and aceruloplasminemia (1). Therefore, the study of copper homeostasis will provide more-in-depth insight into the mechanisms underlying several human diseases. Since yeast cells provide ease in genetic studies, one can take advantage of yeast mutants of the copper homeostatic pathway and yeast genome sequencing data to understand the fundamentals of copper homeostasis.

We have utilized *Saccharomyces cerevisiae* as a model system to understand the regulation of the *CUP1* metallothionein gene. Ace1p drives expression of *CUP1*, allowing rapid production of the MT (i.e., within 10 to 20 min of copper exposure) to protect cells from the toxic effects of copper (16). This induction is achieved by rapid nucleosomal repositioning at the *CUP1* promoter mediated by the RSC (remodel the structure of chromatin) chromatin remodeling complex. The fast cycling of Ace1p and RSC at the *CUP1* locus allows bursts of transcription initiation (16, 17). Involvement of histone H2A and targeted acetylation of histone H3/H4 have been reported at the *CUP1* locus. Furthermore, deletion of acetyltransferase such as Spt10 impairs *CUP1* induction kinetics (18, 19). During the start of *CUP1* induction (within 10 to 20 min), an increase in H3 acetylation occurs, which decreases after 30 min; conversely, H4 acetylation starts increasing, which was not prevalent during the start of the induction process (20). Histone modifications are necessary for both genome-wide transcriptional reprogramming under stress conditions and maintaining steady-state chromatin functions. Individual histone modifications change during stress-induced transcriptional reprogramming (21, 22). For instance, in the case of diamide stress, a majority of the nucleosomes harbor at least one altered modification; a few contain changes in several modifications, and these are enriched at the stress-responsive genes (21). Most of the changed acetylation (ac) marks in H3 (H3K4ac, K9ac, K14ac, K18ac, K23ac, K27ac, and K56ac) and a few methylation (me3) marks (H3K4me3, K36me3, and K79me3) well correlate with transcription activation of reprogrammed genes during diamide exposure (21). Typically, acetylation marks are highly enriched at the 5′ end of stress-induced genes before the increase in RNA abundance, whereas the methylation (especially H3K36me3) level rises at the gene body following transcription initiation (21). Acetylation, however, correlates with gene expression (23–25), and the abundance of acetylated residues (especially H3K23ac) decreases after transcription initiation (24).

Although chromatin remodeler (RSC), acetyltransferase (Spt10), and histone H2A have been implicated in regulating *CUP1* transcription, less is known about how

histone H3 N-terminal tail residues regulate this mechanism. We have provided evidence that histone H3 tail residues regulate *CUP1* transcription by utilizing the library of yeast histone mutants created by Dai et al. (26). We found that N-terminal point mutants H3K23Q, H3K36Q, and H3K27R and truncation mutants H3Δ(13-16), H3Δ(25-28), and H3Δ(28-31) have severe impairment in expressing *CUP1*. We also observed more protein aggregation in copper-sensitive mutants. This could be attributed to the low levels of MT, promoting more protein aggregation. The complementation of *CUP1* partially rescued the growth of these mutants during copper stress. In search of the mechanism behind defective *CUP1* induction in these mutants, we performed chromatin immunoprecipitation (ChIP) to analyze the binding of Ace1 and TATA-binding protein (TBP). ChIP analysis showed that, relative to the wild type, the mutations altering H3 (H3K23Q, K36Q, Δ5-16, Δ13-28, Δ25-28, and Δ28-31) reduced Ace1 occupancy at the *CUP1* promoter. In addition, these mutations also affect TBP binding. We observed an increase in enrichment of the H3K36me3 level upon copper stress at the *CUP1* locus. We further showed that H3 G13-P16 residues are essential for both global and *CUP1* gene-specific H3K9 acetylation. Overall, our results have identified histone H3 residues, and their modifications are required for normal *CUP1* transcription.

RESULTS

Modifiable lysine residues of histone H3 (K23, K27, and K36) are involved in *CUP1* induction. We used mutants of histone H3 and H4 in which the lysine residues were replaced with glutamine, arginine, and alanine that mimic the constitutive acetylated, deacetylated, and unmodified state, respectively. Residues other than lysines were replaced with alanine or glutamic acid. The N-terminal tail mutants of histone H3 and H4 were screened to identify mutants having a defect in copper homeostasis (Fig. 1A and B). Cells with wild-type histone H3 can tolerate up to 2 mM $CuCl_2$, whereas lysine substitution mutation at H3R2, glutamic acid substitution at H3Q5, glutamine substitution at H3 K4, K9, K18, K23, and K36, and H3 Lys27-to-arginine substitution renders cells sensitive to such a high dose of copper (see Fig. S1A and B and Table S1 in the supplemental material). Alanine substitution mutations at H3 Q5, P16, R17, K18, K23, K36, and K(4, 9, 14, 18) residues, which mimic an unmodified state, make cells sensitive to 2 mM $CuCl_2$ (Fig. S1A and B; Table S1). Most of the copper-sensitive mutations clustered in the H3 N-terminal tail residues range from regions 2 to 9 and 16 to 23, while substitutions in the H4 N-terminal tail which are sensitive to copper were not clustered together (Fig. 1A and B). Histone H4 wild-type cells showed normal growth up to 2 mM $CuCl_2$ exposure, whereas the point mutants H4S1D, R3A, K5R, K12Q, K16A, K16Q, K20R, L22A, N25D, and Q27E were found to be sensitive to such a high copper level (see Fig. S2A and B; Table S2). Among them, H4S1D and H4K5R mutants were found to be more sensitive, as they failed to grow normally in even 1 mM $CuCl_2$ concentration (Fig. S2A and B; Table S2). Interestingly, most of the strains that harbored mutations in posttranslationally modifiable residues were found to be copper sensitive, which suggests that histone modifications play a very critical role in copper tolerance. Perhaps, H3 posttranslational modifications (PTMs) are more crucial than those of H4, because alterations of most of the modifiable residues of H3 render cells sensitive to higher copper doses than the wild-type cells.

From the screening, we found substitution mutants H3K23Q, H3K27R, and H3K36Q sensitive to lower copper doses (0.5 to 0.7 mM $CuCl_2$) (Fig. 1C and D), while other substitution mutants showed sensitivity at a much higher copper dose (2 mM $CuCl_2$) (Table S1). The degree of sensitivity also varied with the type of substitution a cell harbored at these residue positions. H3K23Q, which mimics a constitutive acetylated state, is sensitive at 0.7 mM $CuCl_2$, whereas H3K23R and H3K23A, mimicking constitutive deacetylated and unmodified states, respectively, exhibited normal growth during 1 mM $CuCl_2$ exposure (Fig. 1C). This suggests that constitutive acetylation at the H3K23 position hampers the transcriptional program crucial for copper tolerance. Similarly, H3K36R and H3K36A mutants were not sensitive at 1 mM copper, but the H3K36Q mutant exhibited sensitivity at the same dose of copper (Fig. 1C), indicating that

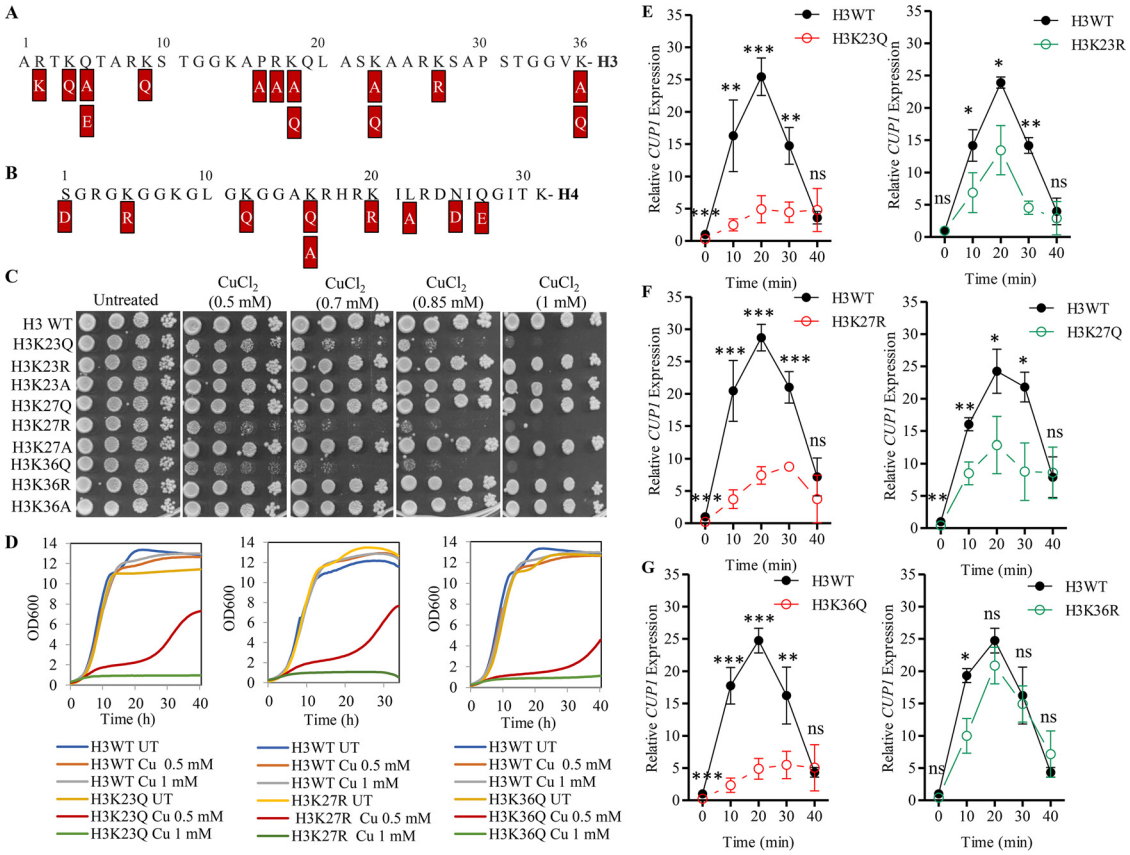

FIG 1 Histone H3 lysine residues are involved in *CUP1* induction. (A, B) Schematic representation of histone H3 and H4 N-terminal tail residues. The amino acid sequences were assigned one-letter codes for respective residues. The substitution mutants found to be sensitive under copper stress (2 mM $CuCl_2$) are shown in boxes. (C) The wild-type and H3 N-terminal point mutant strains were grown overnight, and 10-fold serial dilutions of cells were spotted onto untreated (SC) and copper-containing plates. Plates were incubated at 30°C for 72 h and then scanned. (D) Growth curve analysis of histone H3 wild-type and N-terminal point mutants in liquid culture in the presence and absence of copper ($CuCl_2$, 0.5 mM and 1 mM) compared with those untreated (UT) as a control. For better representation, the growth curves of H3 wild-type (H3WT) cells were kept the same in a few panels, since the growth kinetics was performed simultaneously on the same plate. (E, F, and G) Histone H3 N-terminal point mutants exhibit downregulation of *CUP1* expression. Real-time PCR was performed at the *CUP1* locus, and the *CUP1* transcript levels were normalized with those for *ACT1*. All values are calculated with respect to the C_T (cycle threshold) of the wild-type (WT) uninduced (time zero) samples. Values shown are the means and standard deviations (SDs) from three independent biological repeats (n = 3). Student's t test statistical analyses were performed, and significant differences are indicated as follows: *, $P \leq 0.05$; **, $P \leq 0.005$; ***, $P \leq 0.001$; ns, nonsignificant.

deacetylation of H3K36ac is essential for copper-responsive transcription. Although the H3K36ac mark is enriched at gene promoter regions and associated with transcription initiation (27), its switch to H3K36me3 is also crucial for transcription elongation (21). Generally, the H3K27 methylation mark is associated with repressed promoters (28, 29). We found that the H3K27R mutant, which is defective in K27 acetylation, is sensitive to a low copper dose, but H3K27Q and H3K27A strains showed normal growth during exposure of up to 1 mM copper (Fig. 1C). The sensitivity of these mutants in copper was again validated by growth curve analysis (Fig. 1D). Together, these results suggest that a proper modification state of H3 lysines K23, K27, and K36 is necessary for the cells to maintain copper homeostasis.

The copper-responsive transcription activator Ace1, under excessive copper conditions, upregulates Cup1 expression to protect cells from its toxic effects (30, 31). *CUP1* transcription oscillates upon copper addition: it starts rising and achieves maximum levels within 20 min, and then the level drops subsequently after 20 min. This typical kinetics is required for maintaining a narrow copper window within the cell. Transcriptional regulation of *CUP1* by the histone H2A tail was previously investigated (20) and showed that H2AS2, K5, K120, and K121 residues are required for its normal

induction. As Cup1 is the major copper-detoxifying MT in yeast cells, it is plausible to hypothesize that the hypersensitive mutants such as H3K23Q, H3K27R, and H3K36Q are defective in normal *CUP1* induction. We investigated the *CUP1* expression kinetics in these mutants. Interestingly, the differential copper sensitivity of H3 N-terminal lysine substitution mutants was reflected in terms of relative *CUP1* expression. Mutants that were sensitive to a lower copper dose (H3K23Q, H3K27R, and H3K36Q) exhibited a significant reduction in *CUP1* induction compared to that in wild-type cells (Fig. 1E, F, and G). In contrast, the mutants which were sensitive to a higher copper dose (H3K23R, H3K27Q, and H3K36R) had higher expression of *CUP1* than their sensitive counterparts (Fig. 1E, F, and G). Wild-type cells show maximal *CUP1* induction (25- to 30-fold induction) at around 20 min of copper exposure, whereas the amplitude of *CUP1* expression was reduced nearly five times in H3K23Q and H3K36Q mutants (25.4 [±2.9]-fold induction in the wild type, 4.9 [±2.08]-fold in H3K23Q, and 4.87 [±1.6]-fold in H3K36Q cells) at the same time point (Fig. 1E and G). The maximum *CUP1* induction in H3K27R was achieved after 30 min of copper exposure but was nearly three times less than the level of peak *CUP1* expression in wild-type cells (28.69 [±2.055]-fold induction in wild-type cells at 20 min versus 8.758 [±0.493]-fold induction in H3K27R cells) (Fig. 1F). These results suggest that constitutive acetylation at H3K23 and K36 and a constitutive deacetylation modification state at the H3K27 position hamper normal *CUP1* induction.

Deleting specific regions within the histone H3 tail (5-16, 13-16, 13-28, 25-28, 28-31, and 29-32) confers sensitivity to copper by impairing *CUP1* induction. The neighboring regions of any modifiable residues in the histone H3 tail are also important, as they serve as binding sites for histone-modifying enzymes (32). To find regions in the H3 tail important for higher copper stress, we screened H3 truncation mutants in $CuCl_2$. We found that the majority of H3 truncation mutants were sensitive to 2 mM $CuCl_2$ (see Fig. S3A, B, and C; Table S1), and truncations such as HΔ13-16, Δ13-28, Δ25-28, and Δ28-31 were intolerant to even low copper doses (Fig. 2A). Truncation of H3 13-16, 13-28, and 28-31 residues rendered the cells sensitive to 0.75 mM $CuCl_2$, while truncation of H3 25-28 tolerated a 0.85 mM copper dose (Fig. 2A). We revalidated the sensitivity phenotype of these mutants by growth kinetics analysis and found that H3 13-16 and 13-28 truncation mutants were severely affected, but HΔ(13-16) and H3Δ (13-28) strains showed reduced growth in the presence of 0.5 mM $CuCl_2$ (Fig. 2B). When exposed to a high copper concentration (1 mM $CuCl_2$), only wild-type cells showed normal growth kinetics, whereas truncation mutants were sensitive (Fig. 2B). To find out whether any regions of the H4 tail are important in copper tolerance, we screened H4 tail truncation mutants and found that only a few truncations, notably Δ1-4, Δ1-12, Δ9-12, Δ9-20, Δ13-24, and Δ20-23, were sensitive to a higher copper dose (2 mM) (see Fig. S4A, B, and C; Table S2).

We compared the kinetics of *CUP1* induction in wild-type and truncation mutant cells and found that the *CUP1* expression pattern is consistent with the copper sensitivity phenotype exhibited by these mutants. Truncation of H3Δ(13-16), Δ(25-28), and Δ(28-31) residues drastically reduced the amplitude of *CUP1* induction during copper exposure (Fig. 2C). The H3Δ(13-16) mutant showed both delayed and reduced *CUP1* expression compared to that in wild-type cells. Furthermore, a mutation within residues 13 to 16, such as the substitution of Pro16 with Ala, which hampers H3 tail flexibility, also delayed *CUP1* induction (Fig. 2D). Substitution of proline to alanine (P16A and P30A) conferred sensitivity to a higher dose (Fig. 2E). H3Δ(13-16) cells achieved maximal *CUP1* induction (12.11 [±1]-fold) after 30 min of copper exposure, whereas *CUP1* expression in wild-type cells typically peaked after 10 to 20 min of exposure (Fig. 2C). Most strikingly, the maximum level of *CUP1* induction in H3Δ(25-28) and H3Δ(28-31) strains was around three times less than the peak *CUP1* expression level in wild-type cells [29.39 (±1.96)-fold induction in wild-type, 8.64 (±1.32)-fold in H3Δ(25-28), and 8.88 (±2.08)-fold in H3Δ(28-31) cells] (Fig. 2C). Additionally, several other truncation mutations such as Δ5-16, Δ13-28, Δ29-32, and a long truncation ranging from 4 to 35, which also induced copper sensitivity (Fig. 2F), reduced *CUP1* levels (Fig. 2G). These

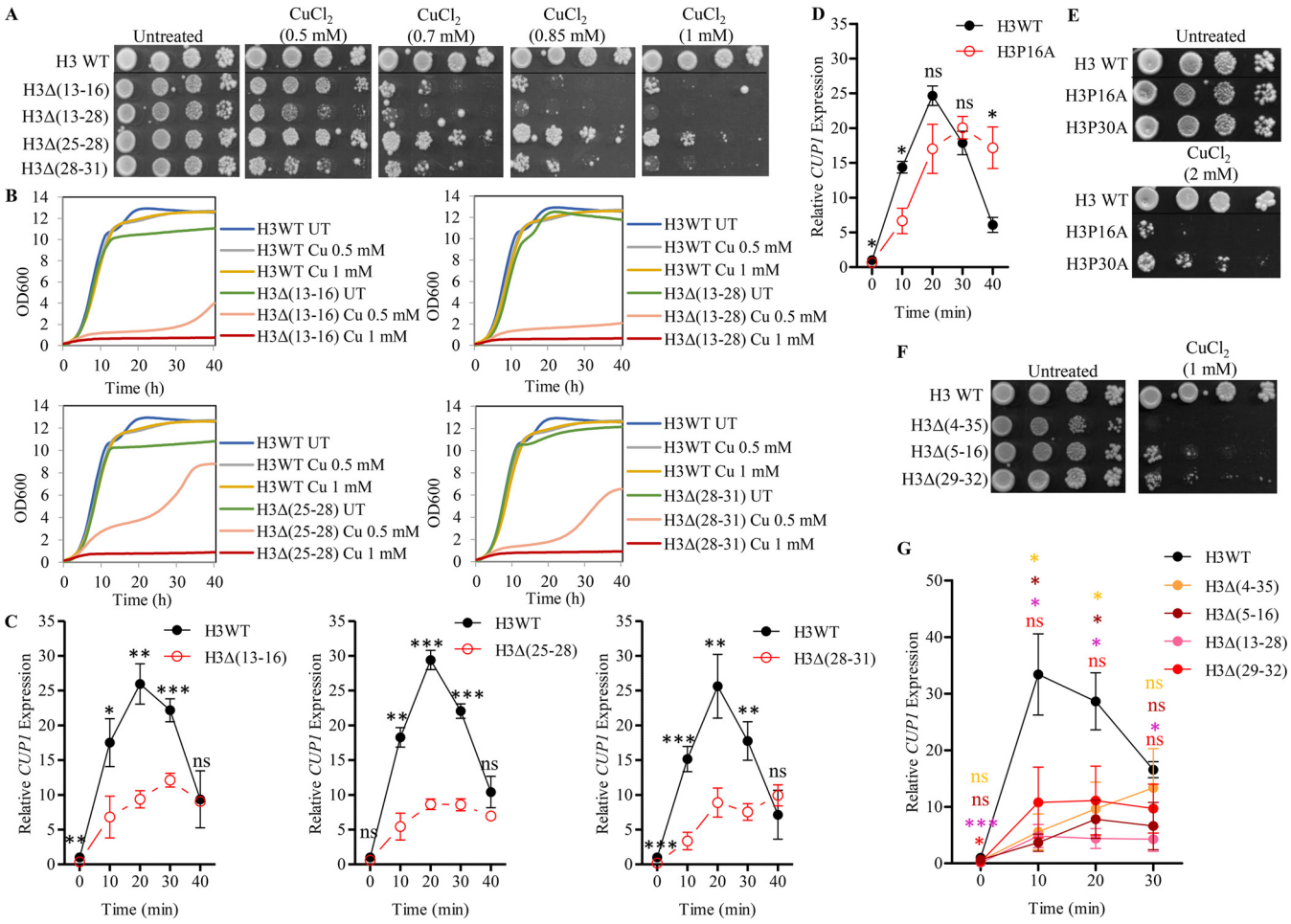

FIG 2 Deletion of specific regions in the histone H3 tail (5-16, 13-16, 13-28, 25-28, 28-31, and 29-32) confers sensitivity to copper by impairing *CUP1* induction. (A) The wild-type and H3 N-terminal truncation mutant strains were grown overnight, and 10-fold serial dilutions of cells were spotted onto untreated (SC) and copper-containing plates. Plates were incubated at 30°C and scanned after 72 h. (B) Growth curve analysis of H3 N-terminal truncation mutants in liquid culture in the presence and absence of copper ($CuCl_2$, 0.5 mM and 1 mM) compared with the untreated wild type (UT) as a control. For easier representation, the growth curves of H3WT cells were kept the same in a few panels, since the growth kinetics was performed simultaneously on the same plate. (C and D) Real-time PCR was performed for the *CUP1* locus, and the *CUP1* expression levels were normalized with those of the internal control, *ACT1*. (E and F) Drop test showing the sensitivity of H3P16A, H3P30A, and H3 truncation mutants in copper. (G) Real-time PCR showing relative *CUP1* expression in H3 truncation mutants compared to that in uninduced H3WT samples. qPCR values were calculated with respect to the C_T (cycle threshold) of the wild-type (WT) uninduced (time zero) samples. Values shown are the means and standard deviations from three independent biological repeats ($n = 3$). Student's *t* test statistical analyses were performed, and significant differences are indicated as follows: *, $P \leq 0.05$; **, $P \leq 0.005$; ***, $P \leq 0.001$; ns, nonsignificant.

results suggest that specific regions of the H3 tail are essential for activation of *CUP1* and might serve as docking sites for transcription activators.

Effects of histone mutations on Ace1 occupancy across the *CUP1* promoter. Next, we hypothesized that specific mutations within histone H3 N-terminal tails affect *CUP1* transcription by altering the binding of Ace1 at the *CUP1* promoter. To test this hypothesis, we performed a ChIP assay and determined Ace1 occupancy at the *CUP1* promoter in copper-sensitive mutants. The activated Ace1 binds at the upstream activation sequence (UAS) region (−177 to −274) of the *CUP1* promoter, and its occupancy was measured at two regions, distal (−182 to −332) and proximal (−1 to −202) to the transcription start site (TSS). A schematic of the *CUP1* locus, along with the known Ace1 binding sites, UAS, and TATA boxes (present at −87 and −134 positions), is shown in Fig. 3A.

Upon copper treatment, Ace1 occupancy increases at both *CUP1-P2* and *P3* regions in H3 wild-type cells. We detected an ~15.2× increase in Ace1 enrichment over that for *CUP1-P3* and an ~8.5× increase in *P2* regions in wild-type cells when exposed to

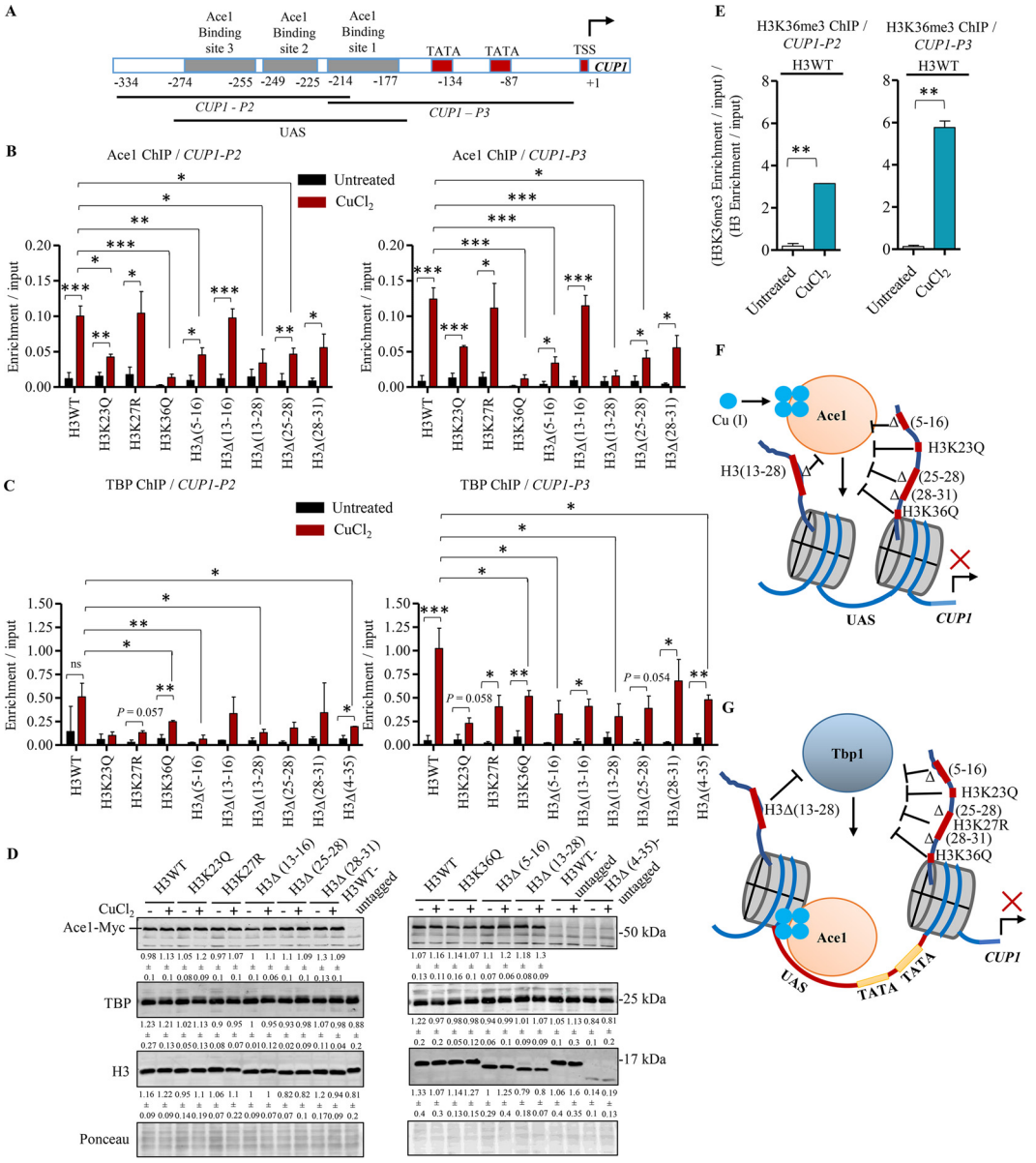

FIG 3 Effects of histone H3 mutations on Ace1 and TBP occupancy across the *CUP1* promoter. (A) Schematic representation of primers used in ChIP along with Ace1 and TBP binding sites at the *CUP1* locus. (B) Graph showing Ace1 occupancy at the *CUP1* promoter in H3 N-terminal mutants relative to that in wild-type cells. Ace1 ChIP analysis shows that mutations of H3 (H3K23Q, K36Q, Δ5-16, Δ13-28, Δ25-28, and Δ28-31) reduce the Ace1 occupancy at both the *CUP1-P2* and *P3* regions. Ace1 ChIP was performed for the *CUP1* promoter using primers *CUP1-P2* and *CUP1-P3* specific for the *CUP1* gene locus. Ace1 binds to both the *CUP1-P2* and *P3* regions upon copper induction, with the highest binding activity at *P3*. (C) TBP enrichment at the *CUP1* promoter upon copper exposure. TBP pulldown was performed in H3WT and H3 mutant cells. qPCR was performed to determine TBP binding at *CUP1-P2* and *P3*. TBP binding was observed more in copper-induced H3WT cells at the *CUP1 P3* region, and overall TBP binding was less in mutants. Ace1 and TBP enrichment was normalized to the amount of input DNA and is shown as enrichment/input (percent). Calculations were performed used the formula $\Delta C_T = C_T$ (ChIP) − [C_T (input) − $\log_{E(2)}$ input dilution factor], where C_T is cycle threshold, E is the specific primer efficiency value, and enrichment/input (percent) = $2^{-\Delta CT}$. Values shown are mean enrichment/input (percent) ± standard errors of the means (SEMs) from three independent biological repeats ($n = 3$). Student's *t* test statistical analyses were performed, and significant differences are indicated as follows: *, $P \leq 0.05$; **, $P \leq 0.005$; ***, $P \leq 0.001$; ns, nonsignificant. (D) Western blot analysis showing global levels of Ace1, TBP, and histone H3 as an internal control for ChIP. The levels of Ace1, TBP, and H3 were normalized with total protein content seen in Ponceau staining using ImageJ. The numbers below each blot represent the averages ± SDs from three independent biological repeats ($n = 3$). (E) H3K36me3 enrichment at the *CUP1* locus upon copper exposure. ChIP showing H3K36me3 enrichment in WT cells at *CUP1-P2* and *P3* during copper stress. H3K36me3 occupancy was normalized with the total H3 enrichment. Values shown are mean H3K36me3/H3 enrichment/input (percent) ± SEMs from two independent biological repeats ($n = 2$). Student's *t* test statistical analyses were performed, and significant differences are indicated as follows: **, $P \leq 0.005$. (F) Model depicting the histone mutants defective in Ace1 binding at the *CUP1* promoter. Mutation of H3K23 and K36 (K23Q, K36Q) and deletion of H3 tail regions 5-16, 13-28, 25-28, and 28-31 hamper Ace1 binding at the *CUP1* promoter. (G) Model summarizing the effect of histone H3 mutations in TBP recruitment over *CUP1* locus. Mutations of H3K23, K27, and K36 (H3K23Q, H3K27R, and H3K36Q) and deletion of H3 tail regions 5-16, 13-28, 25-28, and 28-31 inhibit TBP binding at the *CUP1* promoter.

0.5 mM $CuCl_2$ for 10 min (Fig. 3B). However, we observed no alteration in Ace1 enrichment in H3K27R and H3Δ(13-16) cells upon copper exposure relative to that of wild-type cells. In contrast, the other mutants (H3K23Q, K36Q, Δ5-16, Δ13-28, Δ25-28, and Δ28-31) exhibited reduced Ace1 occupancy in comparison to that of the wild-type cells (Fig. 3B). Two of the strains, H3K36Q and H3Δ(13-28), showed diminished Ace1 occupancy at *CUP1-P3*, whereas H3K23Q, H3Δ(5-16), H3Δ(25-28), and H3Δ(28-31) strains had reduced occupancy, nearly 30% to 45% of the wild-type level (Fig. 3B, right). A similar trend in Ace1 occupancy in mutants was observed at *CUP1-P2*. The reduction in Ace1 enrichment in these mutants is in accordance with the reduced *CUP1* induction seen by real-time quantitative PCR (RT-qPCR) (Fig. 1E and G; Fig. 2C and G) except in H3K27R and H3Δ(13-16) mutants. The H3K27R and H3Δ(13-16) mutations did not affect Ace1 recruitment (Fig. 3B); therefore, it is possible that the reduced *CUP1* induction in these two mutants is due to an impairment in other steps of transcription initiation. Taken together, these results identified residues in H3 that are required to promote Ace1 binding to facilitate *CUP1* transcription.

Histone H3 tail mutations affect TBP binding at the *CUP1* promoter. To further elucidate the cause of low *CUP1* induction in copper-sensitive mutants, we tested the TBP occupancy at the *CUP1* promoter (Fig. 3C). *CUP1* induction requires targeted acetylation of histone H3/H4, which is dependent upon activator (Ace1) and the TATA box. Therefore, TBP binding on the TATA box sequence is crucial for transcription induction (33). TBP enrichment was expected at the *CUP1-P3* (−1 to −202) region, as it contains two TBP binding sites (distal and proximal TATA boxes) and *CUP1-P2* contains no binding site (Fig. 3A). Low levels of TBP binding were also observed in the *CUP1-P2* region in copper-treated cells (Fig. 3C, left), which may be due to PCR amplification of flanking sonicated fragments of variable length along with the *CUP1-P3* region.

Upon copper exposure, the TBP occupancy was increased up to ~22× at the *CUP1-P3* region in H3 wild-type cells, whereas in mutants, TBP binding was substantially less (20% to 50% of the TBP occupancy level in wild-type cells), except for the H3Δ(28-31) mutant (Fig. 3C, right). The levels of TBP1 occupancy in mutants were consistent with the low transcription of *CUP1* seen in these mutants (Fig. 1E to G; Fig. 2C and G). Among these mutations, the H3K23Q mutation led to a severe reduction in TBP binding (decreasing the binding to ~20% of the wild-type level), suggesting that acetylation at the K23 position plays a critical role in TBP recruitment. Contrastingly, TBP enrichment was moderately affected by H3Δ(28-31) mutation (Fig. 3C, right). It might be possible that truncation of H3 28-31 residues affects the recruitment of other chromatin-modifying factors such as the RSC remodeling complex at the *CUP1* locus, thereby hampering nucleosome mobilization. Residues within 28-31 might cross talk with other tail residues such as H3K9, K14, or K36; thus, its truncation may alter overall chromatin structure. Altogether, these results imply that H3K23, K27, and K36 PTMs and residues lying between tail truncations such as 5-16, 13-28, and 25-28 play a crucial role in stress-dependent induction of *CUP1* by promoting proper TBP recruitment. The long truncation ranging from 4 to 35 residues, eliminating most of the tail region, also reduces TBP occupancy. This reaffirms the importance of the H3 tail in TBP recruitment.

To eliminate the possibility that the decreased Ace1 and TBP occupancy could result from downregulation of Ace1, TBP, and histone H3 in mutants, we checked the levels of these factors by Western blot analysis. We observed overall equal protein levels of these epigenetic factors in mutants relative to levels in the wild type, except for the H3Δ(4-35) mutant, wherein the H3 level was drastically reduced (Fig. 3D). This result suggests that expression levels of these factors do not account for the reduced Ace1 and TBP binding in the copper-sensitive mutants.

H3K36 trimethylation is enriched at the *CUP1* locus during copper stress. Trimethylation at H3K36, catalyzed by Set2 in yeast, usually promotes transcription elongation by preventing spurious cryptic transcription (34–36). During oxidative stress, H3K36me3 is highly enriched at Msn2-targeted stress-responsive genes to maintain transcriptional elongation and fidelity (21). However, the function of H3K36me3 in

stress-induced *CUP1* transcription remained unknown. As H3K36Q mutation severely affected Ace1 binding at the *CUP1* locus (Fig. 3B), we wanted to know the importance of H3K36 methylation in *CUP1* induction. We observed an increase in H3K36me3 enrichment at both *CUP1-P2* (~8×) and *P3* (~23×) in wild-type cells under copper stress, coinciding with *CUP1* upregulation (Fig. 3E). This result demonstrates that H3K36me3 is required for *CUP1* expression, and this may account for the defect in *CUP1* induction observed in H3K36Q mutant cells. Besides the enrichment of H3K36me3 at the *CUP1* locus, PTMs such as H3K23 and H4K8 acetylation also showed a global change under copper stress (see Fig. S5A and B), suggesting an alteration in the overall chromatin landscape.

To summarize the findings, we identified H3 N-terminal mutations affecting Ace1 and TBP recruitment at the *CUP1* promoter. Based on our results, we propose a model in which the histone mutations H3K23Q, K36Q, and truncations ranging from residues 5 to 31 (Δ5-16, Δ13-28, Δ25-28, and Δ28-31) lead to impairment in Ace1 recruitment over the *CUP1* promoter during copper stress (Fig. 3F). A majority of the selected mutations also affected TBP binding (Fig. 3G), suggesting that H3 tail residues and PTMs associated with them are critical for optimal recruitment of TBP and thus proper induction of *CUP1*.

H3 N-terminal 13-16 and P16 residues are required for H3K9 acetylation. Generally, H3K9 acetylation promotes transcription initiation (37, 38) by facilitating TFIID recruitment (39). Global H3K9 acetylation is catalyzed primarily by Rtt109 and Gcn5 in *S. cerevisiae* (40). The structure of Gcn5 bound to H3 peptide revealed that during H3K14 acetylation, the amino acids neighboring the substrate residue (G13-P16) play a critical function in stabilizing the interactions between Gcn5 and the R group of K14 (32). Interestingly, we found that G13-P16 residues are also required for the acetylation of H3K9. The global H3K9ac and H3K9acS10P levels were severely reduced (~50%) in H3Δ(13-16) and H3P16A mutant cells in comparison to that in wild-type cells (Fig. 4A and B). The proline 16 residue with *cis-trans* isomerization acts as a hinge point of the H3 tail, and Pro16Ala substitution renders flexibility, thus affecting local tail conformation. This result suggests that G13-P16 residues play an essential role not only in H3K14 acetylation but also in H3K9 acetylation (Fig. 4C).

H3K9 acetylation is associated with stress-induced transcription initiation. The level of H3K9ac at promoters of Msn2 target genes rises during transcription initiation in a stress-dependent manner (21). Evidence also suggests that H3K9ac is enriched at the *CUP1* promoter during copper stress, coinciding with *CUP1* transcription (20, 41). This stress-induced acetylation at *CUP1* is mediated by Spt10, a member of the SAGA acetyltransferase complex (18, 41). As truncation of H3 13-16 and substitution of P16A residues hampers H3K9 acetylation, we therefore suspect that the 13-16 region might be involved in stabilizing Spt10 binding. To check whether this truncation affects Spt10-mediated H3K9 acetylation at *CUP1*, we analyzed H3K9ac and H3 occupancy kinetics at its promoter region. Histone H3 occupancy decreased in wild-type cells within 5 min of copper exposure, indicating proper remodeling of the *CUP1* promoter. The H3Δ(13-16) mutant, however, showed a higher H3 level under normal conditions and a delay in H3 loss at the *CUP1* promoter. We observed a significant difference in H3K9ac enrichment (normalized with total H3 enrichment) between wild-type and H3Δ(13-16) cells during copper exposure. In the wild-type cells, the level of H3K9ac (H3K9ac/H3 enrichment) increased up to 6-fold at *CUP1-P2* and 3.5-fold at the *P3* region within 5 min of copper exposure, whereas in H3Δ(13-16) cells, no such increase in H3K9ac enrichment was observed (Fig. 4D). H3K9 acetylation in the mutant was around 6 to 8 times less than the wild-type level under untreated conditions. In 5 min, the H3K9ac level was ~32- to 43-fold less in the mutant relative to the wild-type level (Fig. 4E). Although a slight increase in H3K9ac in H3Δ(13-16) was seen at 10 min, that increase was not observed at 20 min (Fig. 4E). We speculated that the reduced H3K9ac level was likely the cause of the *CUP1* transcription defect. To our surprise, both Ace1 and TBP were highly enriched at 5 min of copper exposure, whereas in wild-type cells, Ace1 and TBP achieved maximum

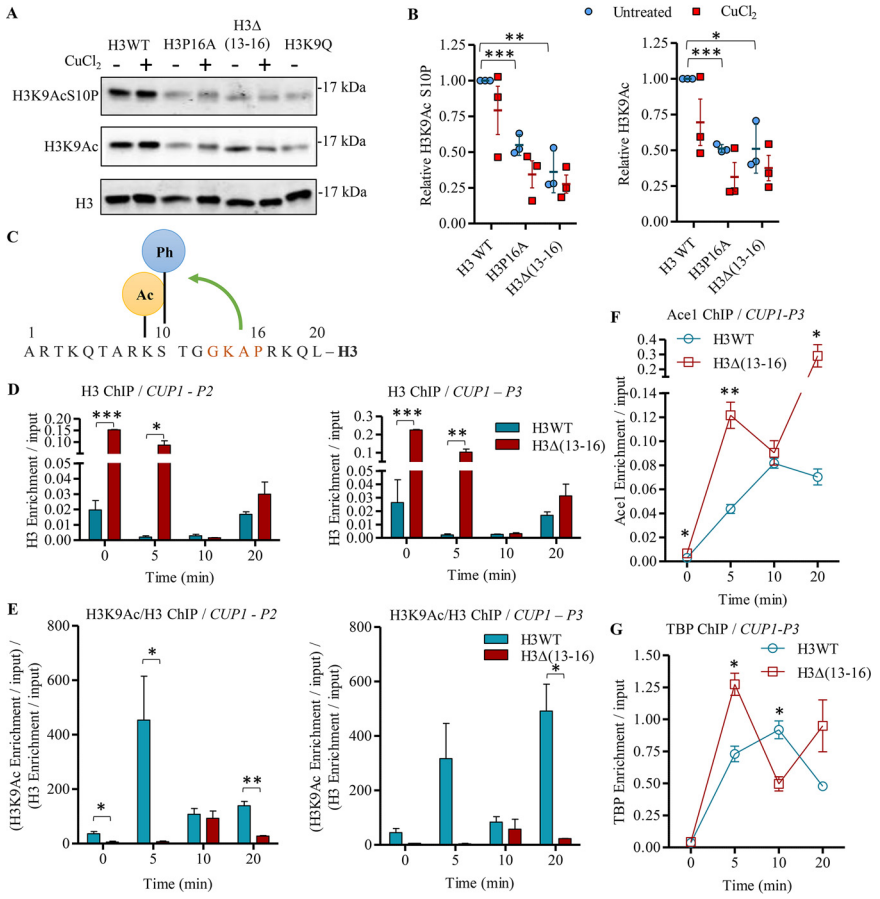

FIG 4 H3Δ(13-16) mutation reduces H3K9 acetylation level and alters Ace1 and TBP kinetics at the *CUP1* locus. (A) Truncation of H3 13-16 and substitution mutation P16A reduce global H3K9 acetylation. Western blot examining global histone modifications H3K9 acetylation and H3K9acS10P in H3WT and H3Δ(13-16) and H3P16A mutants with and without copper induction. Histone H3 is taken as a loading control, and H3K9Q is taken as a negative control. (B) H3K9acS10P and H3K9ac were quantified using ImageJ, and the values were normalized with total H3 that serves as a loading control and depicted in the form of a scatterplot. Values represent the means ± SEMs from three independent biological repeats ($n = 3$). Student's *t* test statistical analyses were performed, and significant differences are indicated as follows: *, $P \leq 0.05$; **, $P \leq 0.005$; ***, $P \leq 0.001$. (C) Schematic showing cross talk among histone H3 residues P16 and K9ac. (D) ChIP showing histone H3 occupancy kinetics in H3WT and H3Δ(13-16) mutant at the *CUP1* locus. Histone H3 enrichment decreases with time upon copper treatment in H3WT cells, whereas in H3Δ(13-16) mutants, H3 loss is delayed. (E) ChIP analysis showing H3K9 acetylation kinetics upon copper exposure at the *CUP1* locus. H3K9ac levels drastically increased in H3WT cells under copper stress, whereas they were significantly reduced and delayed in H3Δ(13-16) mutants. H3K9ac enrichment was normalized with the total H3 enrichment. Values shown are mean H3 and H3K9ac/H3 enrichment/input (percent), and error bars denote SEMs from three independent biological repeats ($n = 3$). Student's *t* test statistical analyses were performed, and significant differences are indicated as follows: *, $P \leq 0.05$; **, $P \leq 0.005$; ***, $P \leq 0.001$. (F and G) ChIP showing Ace1 and TBP enrichment kinetics at the *CUP1-P3* region in H3WT and H3Δ(13-16) cells. The Ace1 and TBP enrichment values were normalized with the input DNA. Values shown are mean enrichment/input (percent) ± SEMs from three independent biological repeats ($n = 3$). Student's *t* test statistical analyses were performed, and significant differences are indicated as follows: *, $P \leq 0.05$; **, $P \leq 0.005$.

binding at 10 min (Fig. 4F and G). There is a possibility of defective binding of some other epigenetic factors, but at this point, we are unable to resolve the *CUP1* induction defect in this mutant.

***CUP1* complementation in H3 tail mutants partially rescues copper sensitivity.** Since copper-sensitive histone H3 mutants exhibit downregulation of *CUP1*, we wondered if *CUP1* overexpression could rescue the copper sensitivity in these mutants. To check the rescue of copper sensitivity, we cloned *CUP1* under the control of the inducible *GAL1* promoter. We transformed the copper-sensitive H3 mutants with p*GAL1*-

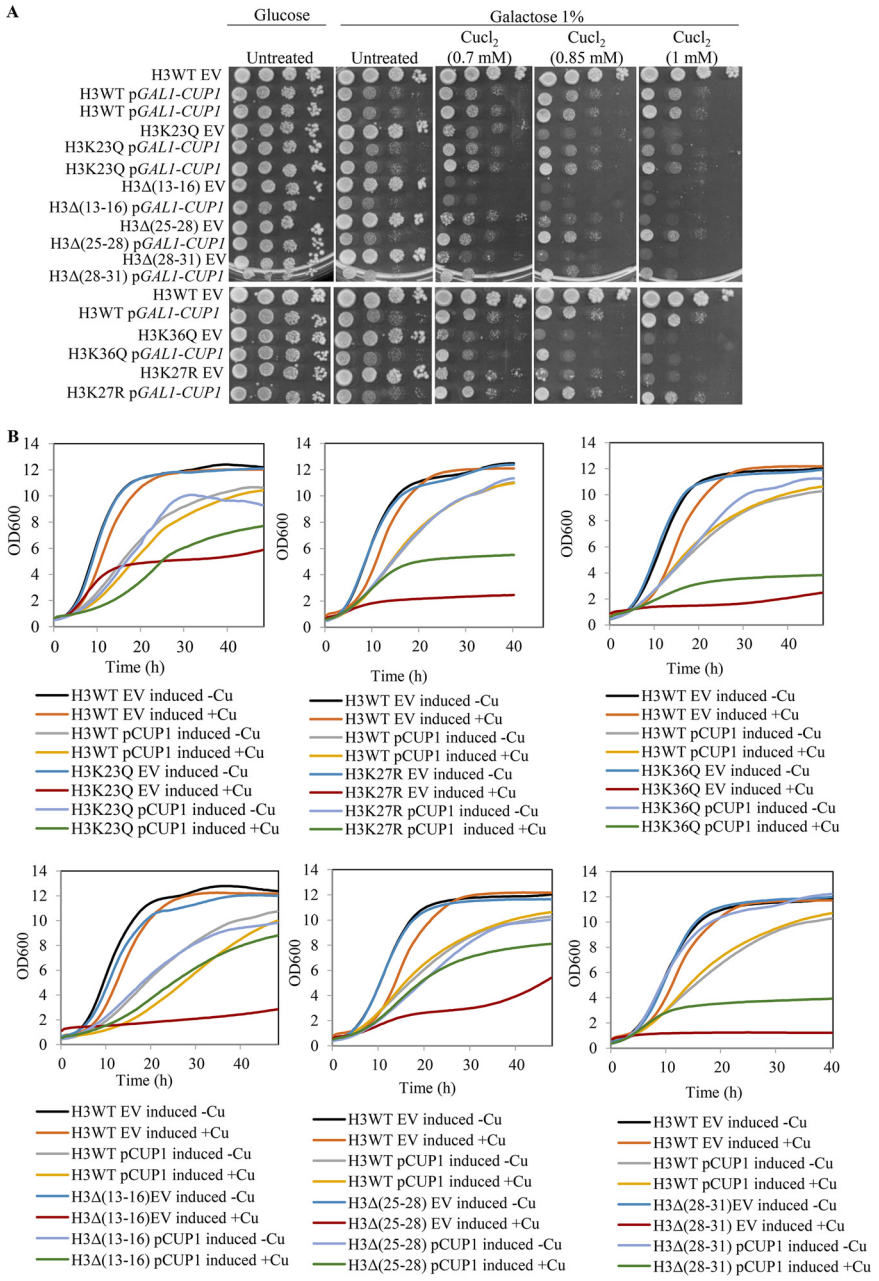

FIG 5 *CUP1* complementation rescues the copper sensitivity phenotype of histone H3 N-terminal mutants. (A) Tenfold serial dilutions of cells were spotted onto uninduced (SC-Leu plus glucose) and induced (SC-Leu plus galactose) copper-containing plates. Plates were incubated at 30°C and scanned after 72 h. (B) Growth curve analysis of p*GAL1-CUP1* (indicated as p*CUP1*)-complemented clones and empty vector in liquid culture. Clones were grown under a *GAL1* induced (SC-Leu plus 2% galactose) condition with or without copper treatment. Induced clones were treated with different copper doses [H3K23Q, H3Δ(13-16), and H3Δ(25-28) were treated with 0.25 mM $CuCl_2$; H3K27R, H3K36Q, and H3Δ(28-31) were treated with 0.5 mM $CuCl_2$] and plated in 96-well plates for growth kinetics measurement up to 48 h.

CUP1 or vector only as a control (EV), and *CUP1* expression was validated by Western blot analysis (see Fig. S6A and B). We observed the rescue of *CUP1*-complemented mutant clones under copper stress, whereas the mutants having empty vector failed to tolerate this stress (Fig. 5A). Lysine-substituted mutants such as H3K23Q, H3K27R, and H3K36Q were rescued at $CuCl_2$ 0.85 mM, and deletion mutants H3Δ(13-16), H3Δ(25-28), and H3Δ(28-31) showed rescued growth at 0.7 mM when complemented with

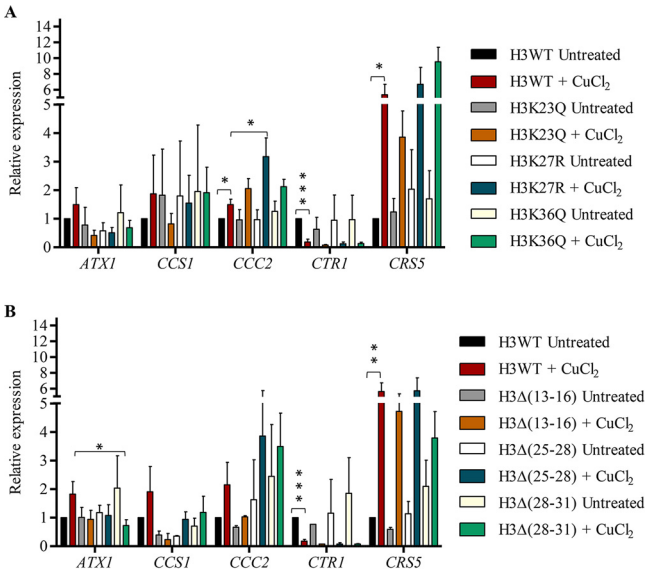

FIG 6 Effect of H3 tail mutations on copper homeostasis genes. Expression of copper homeostatic genes in H3WT and copper-sensitive histone mutants is shown. All gene expressions were normalized with *ACT1* expression level. Fold change was calculated using the formula $2^{-\Delta\Delta CT}$, where $\Delta\Delta C_T$ is ΔC_T (test gene) − ΔC_T (control gene). Values represent the means ± SEMs from three independent biological repeats ($n = 3$). Student's *t* test statistical analyses were performed, and significant differences are indicated as follows: *, $P \leq 0.05$; **, $P \leq 0.005$; ***, $P \leq 0.001$.

CUP1 (Fig. 5A). The rescue upon *CUP1* complementation observed in the mutant cells was further validated by performing growth kinetics (Fig. 5B). Galactose-induced *CUP1* clones of H3K27R, H3Δ(13-16), H3Δ(25-28), and H3Δ(28-31) displayed significant growth rescue in copper (Fig. 5B). On the other hand, *CUP1*-complemented clones of H3K23Q and H3K36Q exhibited less rescue in copper (Fig. 5B). Furthermore, variable degrees of rescue were observed in different mutant clones, which were probably due to their differential sensitivities in copper.

Effect of H3 tail mutations on copper homeostasis genes. Complementation of *CUP1* in N-terminal mutant cells of histone H3 partially rescued the copper sensitivity, indicating the possibility of a defect in some other genes associated with the copper homeostatic pathway. To assess the defect in genes of the copper homeostatic pathway, we checked the expression of genes involved in the export, delivery, or chelation of copper (Fig. 6). In the case of the gene encoding a copper chaperone, *ATX1*, the expression remained unaltered in all strains (Fig. 6). The mRNA level of *CCC2* (encoding a P-type ATPase) was higher in H3Δ(25-28) and H3Δ(28-31) mutants than in wild-type cells upon copper exposure (Fig. 6B). However, in H3Δ(13-16) cells, the expression levels of *CCC2* and *CCS1* (Cu chaperone for SOD1) were reduced (Fig. 6B). This reduced *CCS1* is indicative of more oxidative stress in this mutant, since the active form of *SOD1* is required during oxidative stress and *CCS1* functions in the activation of *SOD1* (42). The *CTR1* gene usually undergoes downregulation upon copper stress to prevent excess uptake of copper; no abnormality in *CTR1* repression was seen in the mutants.

Most of the mutants induced *CRS5* upon copper stress to the wild-type level, except H3K23Q and H3Δ(28-31). The *CRS5* induction may be a compensatory strategy of cells to cope with the downregulation of *CUP1*, since *CRS5* is the minor metallothionein that is induced upon copper exposure. Both the MTs (*CUP1* and *CRS5*) are under the regulation of Ace1p, but *CRS5* contains only a single Ace1p binding site. Yeast strains having downregulated *CUP1* display some degree of copper resistance, which is probably mediated by *CRS5* (2, 43, 44).

Copper causes protein aggregation in histone tail mutants. Several transition metals such as arsenic (45) and cadmium (46, 47) are known inducers of intracellular protein aggregation. Aggregation of nascent polypeptides or misfolded proteins inside

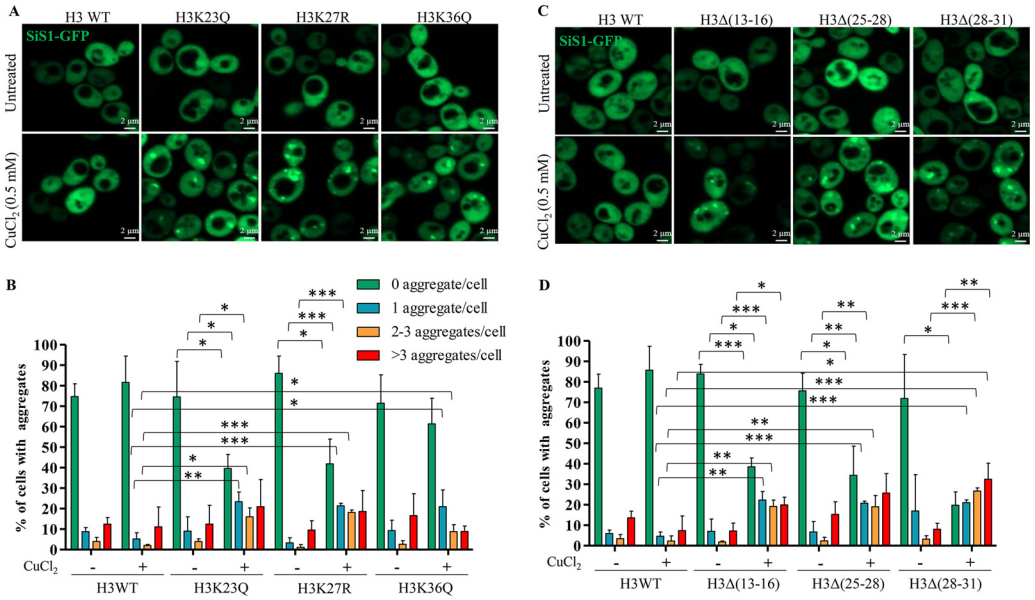

FIG 7 Copper induces protein aggregation in H3 tail mutants. (A and C) Visualization of protein aggregation using Sis1-GFP reporter by fluorescence microscopy. H3WT and copper-sensitive histone mutant cells transformed with Sis1-GFP plasmid. Transformants were grown until mid-log phase, treated with 0.5 mM $CuCl_2$ for 1 h, and subjected to microscopy. Representative images for H3WT and each mutant are shown. (B and D) Quantification of Sis1-GFP aggregates. Sis1-GFP distribution was scored in H3WT and mutant cells. Percentage of cells containing aggregates were categorized into 3 classes, 1 aggregate/cell, 2 to 3 aggregates/cell, or >3 aggregates/cells, by visual inspection using ImageJ software. Cells were counted, and values represent means ± SEMs from 3 independent biological repeats ($n = 3$). Student's *t* test statistical analyses were performed, and significant differences are indicated as follows: *, $P \leq 0.05$; **, $P \leq 0.005$; ***, $P \leq 0.001$.

the endoplasmic reticulum is one of the major cytotoxic effects of these metals. It has been reported that copper causes aggregation of ubiquitin protein by affecting its stability (48). Similar studies have shown the effect of Cu(II) ions on alpha-synuclein aggregation (49). Altogether, these studies have highlighted the potential of copper ions to promote protein aggregation and fibril formation. To find out the cytotoxic effect of dysregulated copper sequestration in yeast histone mutants, we looked into the formation of intracellular protein aggregates in copper-sensitive mutants. We visualized the copper-induced protein aggregates using the Sis1-green fluorescent protein (GFP) reporter plasmid. Sis1 cochaperone proteins associate with unfolded protein aggregates and either facilitate their disaggregation or transport them for nuclear degradation (50–52). Normally, Sis1 cochaperones are evenly distributed throughout the nucleus and cytosol, but they accumulate with protein aggregates. These aggregation sites can be seen as foci of Sis1-GFP (50). We transformed wild-type and copper-sensitive mutants with p*ADH1-SIS1-GFP* plasmid and observed protein aggregation upon copper exposure. Cytosolic foci were formed in all copper-sensitive mutants when exposed to 0.5 mM $CuCl_2$ for 1 h, whereas most of the wild-type cells (83.67% ± 11.2%) were devoid of any cytosolic aggregates (Fig. 7). We observed that a majority (~60% to 80%) of mutant populations [60.3% ± 6.7% of H3K23Q, 58.14% ± 12.1% of H3K27R, 61.4% ± 4.31% of H3Δ(13-16), 65.6% ± 14.2% of H3Δ(25-28), and 80.1% ± 6.4% of H3Δ(28-31) cells] had at least one aggregation site during copper exposure, while only 16% ± 11.2% of wild-type cells exhibited protein aggregates (Fig. 7B and D). The H3K36Q mutant, however, showed less protein aggregation than other mutants, as only 38% ± 12.5% of the copper-exposed cells contained at least one protein aggregate (Fig. 7A and B). Furthermore, the proportion of cells containing 2 to 3 or >3 aggregates was higher for all sensitive mutants (~36% to 60%) than for the wild type (~11%) (Fig. 7B and D). Together, these results suggest that dysregulation of copper homeostasis impairs protein folding and quality control, which may be one of the reasons for the sensitivity of these mutants.

DISCUSSION

Normal kinetics of *CUP1* induction requires a complex interplay between the transcription factors, histone-modifying enzymes, and chromatin remodeling complex. Evidence suggests that the involvement of histone H2A residues and acetylation marks at H3 and H4 are essential for *CUP1* induction and autoregulation (18, 20). However, the role that each residue on the tail regions of histone H3 and H4 plays during *CUP1* induction is not known. Our screening helped to gain insight into histone tail-mediated *CUP1* regulation. The fact that a majority of sensitive mutations are the substitution of modifiable residues (Fig. 1A and B) indicates that the PTMs associated with histone tails play a critical role in activating copper-responsive genes. Substitution mutations of modifiable lysines in H3 (H3K23Q, H3K27R, and H3K36Q) and truncation of specific regions of the H3 tail (Δ5-16, Δ13-16, Δ13-28, Δ25-28, Δ28-31, and the long truncation Δ4-35) significantly reduced the intensity of *CUP1* induction (Fig. 1E, F, and G and Fig. 2C and G). Activation of *CUP1* requires Ace1-mediated nucleosome repositioning at the promoter region, which makes the chromatin accessible for transcription machinery (53). Our results show that many copper-sensitive mutations reduce Ace1 binding at response elements in the *CUP1* promoter under copper stress (Fig. 3B). This reduction in Ace1 occupancy may be a primary cause for faulty *CUP1* induction in these mutants. However, we cannot ignore other steps in Ace1-mediated transcription initiation. Unlike for other genes where an increased resident time of transcription factors improves their induction (54–56), improvement of *CUP1* transcription correlates with a decrease in Ace1 resident time (16, 57). Although Ace1 binds very transiently, its fast cycling at the promoter leads to transcription bursts of *CUP1* (16, 17, 57). Thus, it will be interesting to investigate whether the cycling of Ace1 is affected in these sensitive histone mutants. Furthermore, the RSC chromatin remodeling complex facilitates Ace1 cycling by repetitively mobilizing the −1 nucleosome at the *CUP1* promoter (17). The effect of these histone mutations in RSC-mediated nucleosome mobilization needs to be investigated.

Binding of Ace1 at the *CUP1* promoter triggers the formation of a preinitiation complex comprising of TBP, TFIIB, and RNA polymerase II (58). The recruitment of TBP correlates with transcriptional activation (58). We show that a majority of the mutations decrease TBP occupancy at the TATA boxes present in the *CUP1* promoter during copper stress, which is more prominent in H3K23Q, H3Δ(5-16), and H3Δ(13-28) mutants (Fig. 3C). This decrease in TBP occupancy is one of the reasons for low *CUP1* induction in mutants. It has been demonstrated that hyperacetylation of H3 and H4 occurs at the time of TBP recruitment by Spt10 (18). However, it is debatable whether TBP binding promotes acetylation or vice versa. We speculate that loss of acetylation marks in these mutants might be the reason for the reduction of TBP occupancy.

The level of H3K9 acetylation at the *CUP1* promoter correlates with *CUP1* induction (20). Consistent with this, we observed an increase in H3K9ac at the *CUP1* promoter in wild-type cells under copper stress. On the contrary, truncation of H3 13-16 residues hampered H3K9 acetylation at the *CUP1* promoter under copper stress. Furthermore, it affected global H3K9ac, suggesting cross talk between H3 13-16 residues and the H3K9 acetylation mark. The H3P16A mutation, which hinders the flexibility of the tail, also had the same effect on global H3K9ac, indicating that *cis-trans* isomerization of P16 is essential for acetylation at the H3K9 residue. Further investigation is needed to gain mechanistic insights into this cross talk. Besides H3K9ac, we found that H3K36 trimethylation also increased at the *CUP1* promoter during copper stress. Involvement of H3K36me3 in *CUP1* induction was unknown. This result is consistent with the observation that H3K36me3 is often associated with transcriptionally active genes (21, 59–62). Probably, H3K36me3 enrichment at the *CUP1* promoter is required to prevent aberrant transcription initiation, as evident from previous studies (36, 63, 64).

Cup1 protein sequesters intracellular copper ions to prevent toxicity. The gene expression results show that copper-sensitive histone mutants fail to induce *CUP1* compared to that of wild-type cells. Therefore, with the rationale that restoration of

CUP1 transcript levels in these mutants would rescue their growth during copper stress, we complemented these cells with exogenous *CUP1*. As expected, *CUP1* complementation rescued these mutants during copper stress, although it was a partial rescue (Fig. 5). Thus, in the presence of exogenously introduced *CUP1*, cells acquire the ability to tolerate copper excess due to increased sequestration and detoxification capacity. However, the rescue may have been incomplete because excessive Cup1 is detrimental for normal growth. Alternatively, since histone residues regulate global transcription, the expression of multiple genes involved in copper homeostasis may be affected in these mutants.

Excessive copper accumulation has been linked with protein aggregation. Copper binds to alpha-synuclein and promotes its aggregation in the brain (65–67). To find out the cytotoxic effect associated with Cup1 deficiency in histone mutants, we visualized the copper-induced protein aggregation (50). The appearance of Sis1-GFP puncta in mutants upon copper exposure (Fig. 7) suggests that protein aggregation is one of the manifestations of defective copper homeostasis.

A recent study demonstrated that H3-H4 acts as an enzyme for reducing the nonbiousable Cu^{2+} to biousable Cu^{1+} *in vitro*. The H113 and C110 residues provide the interface for cupric ion binding (68). As an alternative perspective, the H3 tail might be involved in stabilizing the H3-H4 tetramer to perform its reductase function. Alteration of the tail may disrupt the H3-H4 tetramer and affect this function. It is evident that Ace1 gets activated by the Cu^{1+} ion. Activated Ace1 is required to activate *CUP1* transcription. Therefore, low bioavailability or failure of the cells to reduce Cu^{2+} to the Cu^{1+} ion will hamper Ace1 activation and reduce *CUP1* transcription.

In summary, our study has uncovered the role of a few histone H3 residues in the regulation of *CUP1* gene transcription. *CUP1* induction levels were associated with tolerance toward copper stress; thus, histone mutants having defective *CUP1* gene expression cannot tolerate copper stress (Fig. 8).

MATERIALS AND METHODS

Yeast strains, plasmids, and growth conditions. The strains used in this study are synthetic histone H3/H4 mutant library strains created by Dai et al. (26) and commercially purchased from Dharmacon (Lafayette, CO; catalog number [cat. no.] YSC5106); they are listed in Table S3 in the supplemental material. The metal sensitivity drop test was conducted in synthetic complete (SC) medium (containing all amino acids, 0.17% yeast nitrogenous base, 0.5% ammonium sulfate, and 2% glucose; 2% Bacto agar was added for SC plates). Copper chloride dihydrate ($CuCl_2{\cdot}2H_2O$) was purchased from Sigma (cat. no. 307483).

Ace1-myc tagged yeast strains were generated using pFA-6a-13 myc plasmid with the URA3 marker gene by integrating 13-myc tag at the 3′ end of *ACE1* (69). p*GAL1-CUP1* was generated by cloning *CUP1* gene between BamHI and SalI sites in p425-*GAL1-SSE1* (70), removing *SSE1*, and inserting *CUP1*. p*GAL1-CUP1* clones were confirmed by colony PCR, sequencing, and Western blotting using an anti-His antibody. *pAG415-ADH1-SIS1-GFP* (50) used for visualizing protein aggregates was gifted from Simon Alberti.

Phenotypic analysis. Drop test analysis was conducted by preparing 10-fold serial dilutions of each strain, and 3 μl of H3WT cells and mutants was spotted onto SC agar plates untreated or containing different doses of $CuCl_2{\cdot}2H_2O$. Growth assessment was performed after 72 h of incubation at 30°C.

Growth sensitivity of the cells was validated in liquid culture using a microplate reader (Biotek Instruments, Inc., USA), in 96-well plates after a predetermined duration. Cells were grown until the mid-log phase, set to an optical density (OD) of 0.2, before treating the cells with predetermined copper doses (0.5 mM, 1 mM, and 2 mM). Graphs were generated by analyzing the data values in MS-Excel.

***CUP1* induction experiments and real-time qPCR.** *CUP1* induction was carried out by growing cells up to mid-log phase (OD range between 0.8 and 1); then, 0.5 mM $CuCl_2{\cdot}2H_2O$ was added and cells were incubated at 30°C. To monitor the *CUP1* induction kinetics, cells were harvested at different time points (0, 10, 20, 30, and 40 min) after copper addition. Total RNA extraction was carried out by the hot-phenol method (71), and 1 μg of RNA was used for cDNA preparation using an iScript cDNA synthesis kit (Bio-Rad; cat. no. 1708891). Standard protocols were used for real-time PCR (KAPA; cat. no. KK4618). Expression of *CUP1* and other genes was normalized to that of an internal control, *ACT1*. Primers used for gene expression analysis are listed in Table S4.

Western analysis. Exponentially growing cells were harvested and washed with trichloroacetic acid (TCA). Whole-cell protein extraction was carried out by using a standard protocol with slight modification (72). Cells were resuspended in 200 μl of 20% TCA, and 0.5-mm glass beads were added and vortexed for 10 min at room temperature (RT). The lysate was collected in another tube by piercing the tubes from the bottom. Then, the lysate was centrifuged for 10 min at 7,000 rpm, and the supernatant was discarded. The protein pellet was washed using 0.5 M Tris-Cl (pH 7.5). The supernatant was

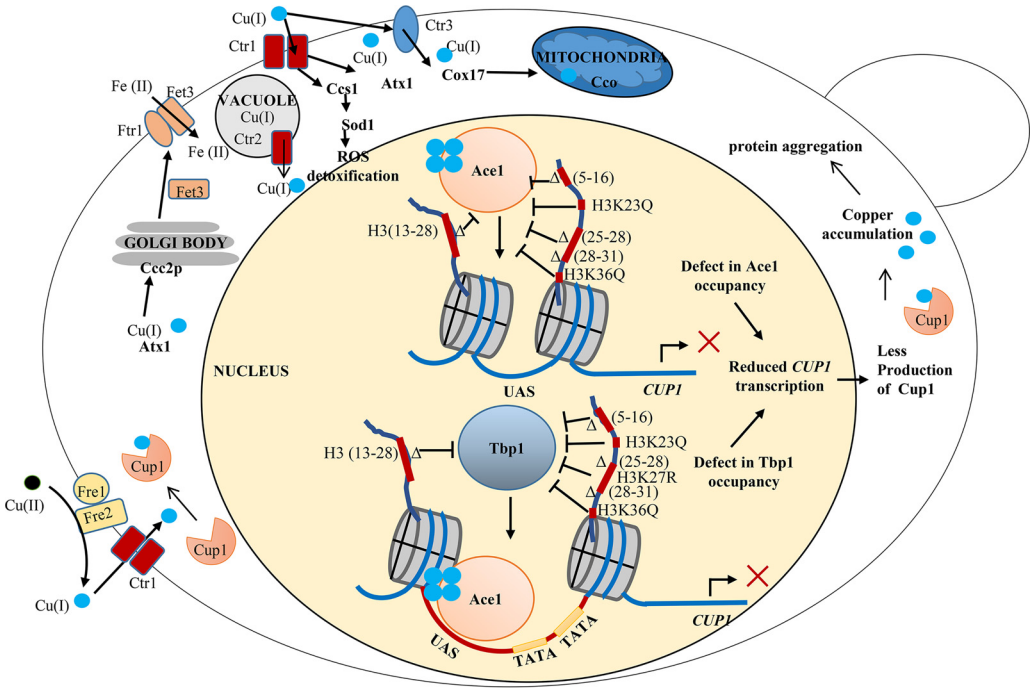

FIG 8 Pathways involved in copper homeostasis in *S. cerevisiae* and the role of N-terminal tail residues of H3 in regulating *CUP1* induction. Copper uptake is facilitated by transporters and ferric reductases (Ctr1, Ctr3, and Fre1/2), and upon internalization, copper is delivered to its target sites by key copper chaperones (Ccs1, Atx1, and Cox17). Copper is then utilized in various cellular processes, and enzymes such as SOD1 and CCO1 require copper as a cofactor. When the concentration of copper increases inside the cells, the copper detoxification pathway mediated by Cup1 and Crs5 MTs is induced. These MTs chelate copper to prevent toxicity. Cup1 MT is transcriptionally regulated by activator protein Ace1 under copper excess conditions. We found that the mutations at the N-terminal tail region of histone H3 hamper Ace1 and TBP binding during *CUP1* induction; thus, cells fail to produce a sufficient amount of Cup1 MT. Excessive amounts of intracellular copper trigger protein aggregation.

removed, and the pellet was dissolved in 0.5 M Tris-Cl and 6× SDS loading dye. Samples were boiled at 100°C for 10 min, followed by centrifugation at 13,000 rpm for 10 min. Immunoblotting was performed by taking equal amounts of whole-cell extract (WCE) resolved on SDS-PAGE gel and blotting onto the nitrocellulose membrane using a wet-electrotransfer system. Antibodies used in the Western blot analysis were anti-myc (9E-10) and anti-His (gifted from Ram Kumar Mishra), anti-TBP (polyclonal sera generated in our lab), anti-TBP ChIP grade (gifted from Joseph C. Reese), anti-H3 (Sigma-Aldrich; H0164), anti-H4 (SAB4500312), anti-H3K9ac (Abcam; ab69830), anti-H3K9acS10P (Sigma-Aldrich; H9161), anti-H4K8ac (Abcam, 15823), anti-mouse IgG secondary antibody (926-32210), and anti-rabbit IgG secondary antibody (A32734). Blots were scanned under an Odyssey infrared imager (LI-COR Biosciences). The intensity of H3, H3K9ac, and H3K9acS10P bands was quantified by using ImageJ software.

Chromatin immunoprecipitation. Cells were grown in selection medium (Trp^-) up to mid-log phase, induced with 0.5 mM $CuCl_2$ (treated), and allowed to grow for 10 min. Cross-linking was performed with 1% formaldehyde for 15 min at 25°C, followed by quenching using glycine for 5 min. Cells were harvested, washed, and resuspended in FA lysis buffer (50 mM HEPES, 150 mM NaCl, 2 mM EDTA, 1% Triton X-100, 0.1% sodium deoxycholate, 0.1% SDS, protease inhibitor cocktail, and phenylmethylsulphonyl fluoride). Mechanical lysis was performed by using equal amounts of 0.5-mm glass beads and briefly vortexing for 30 s followed by keeping on ice for 30 s, up to 5 times each. Sonication was carried out using a Diagenode Bioruptor for 15 cycles of 30 s on/off. Following sonication, lysate clearing was performed by centrifuging for 30 min at maximum speed at 4°C. Of the total sonicated lysate (WCE), 100 μl was taken as "input" and the rest was stored at −80°C for other IPs. The average size of sheared chromatin ranged from 200 to 600 bp. Chromatin immunoprecipitation was carried out overnight at 4°C by incubating chromatin with 30 μl bead slurry (Dynabead protein G, cat. no. 10003D; Thermo Fisher Scientific) conjugated for 2.5 h at 4°C on a rotamer with the following antibodies: anti-myc (9-E-10), anti-H3K9ac (Abcam; ab69830), anti-histone H3 (Abcam; ab1791), anti-H3K36me3 (ABE435S), and anti-TBP (gifted from J. C. Reese). Washing of immunoprecipitated chromatin was performed under stringent conditions using the following buffers: low-salt buffer (0.1% Triton X-100, 2 mM EDTA, 0.1% SDS, 150 mM NaCl, 20 mM HEPES), high-salt buffer (0.1% Triton X-100, 2 mM EDTA, 0.1% SDS, 500 mM NaCl, 20 mM HEPES), LiCl buffer (0.5 M LiCl, 1% NP-40, 1%, sodium deoxycholate, 100 mM Tris-Cl [pH 7.5]), and 1× Tris-EDTA (TE) buffer (pH 8). One hundred microliters of WCE was taken as input control. A de-cross-linking step was performed at 65°C overnight. DNA isolation was carried out from both IP and input samples as described previously (73). qPCR was performed using SYBR green mix (KAPA Biosystems; cat. no. KK4618). Ace1 enrichment was normalized to the amount of input DNA and is represented as enrichment/

input (%) (17). All the calculations were performed using the formula $\Delta C_T = C_T(\text{ChIP}) - [C_T(\text{input}) - \log_{E(2)}(\text{input dilution factor})]$, where C_T is cycle threshold; enrichment/input (percent) = $2^{-\Delta CT}$ (17). The ChIP experiments were conducted at least twice.

Fluorescence microscopy. Wild-type and copper-sensitive mutants were transformed with plasmid *pAG415-ADH1-SIS1-GFP*. Transformed cells were grown in SC medium lacking leucine (SC-Leu medium) until mid-log phase (OD_{600} of ~0.6) and treated with 0.5 mM $CuCl_2$ for 1 h. Cells were harvested and then washed with 1× phosphate-buffered saline (PBS). Images were captured under ×63 magnification using a Zeiss-Apotome.2 fluorescence microscope (Zeiss, Jena, Germany). The λ excitation/λ emission for GFP is 488 nm/509 nm. Images were processed using ZEN Pro 2012 software. Cells containing Sis1-GFP puncta were counted (using ImageJ) and categorized into four groups (0, 1, 2 to 3, and >3 aggregates/cell).

SUPPLEMENTAL MATERIAL

Supplemental material is available online only.

SUPPLEMENTAL FILE 1, PDF file, 1.5 MB.

ACKNOWLEDGMENTS

We thank Simon Alberti and Helen Saibil for providing us with the p*AG415-ADH1-SIS1-GFP* and p*425-GAL1-SSE1* plasmids, respectively. All the members of the Chromatin Biology Laboratory-IISER Bhopal are acknowledged for helpful discussions throughout this work. Rohit Kumar and Anaswara Sugathan are acknowledged for assistance.

This work was supported by funds from the Council of Scientific and Industrial Research, Government of India [CSIR grant no. 38(1468)/18/EMR-II] to R.S.T. and intramural funds from IISER Bhopal. S.S. and R.K.S. received fellowship support from CSIR and IISER Bhopal, respectively.

We declare no conflicts of interest.

S.S., R.K.S., and R.S.T. designed the study. S.S. and R.K.S. performed the experiments and analyzed results along with R.S.T. S.S. and R.K.S. prepared all the figures. S.S., R.K.S., and R.S.T. wrote the paper. All authors reviewed the results and approved the final version of the manuscript.

REFERENCES

1. Nevitt T, Ohrvik H, Thiele DJ. 2012. Charting the travels of copper in eukaryotes from yeast to mammals. Biochim Biophys Acta 1823:1580–1593. https://doi.org/10.1016/j.bbamcr.2012.02.011.
2. Culotta VC, Joh HD, Lin SJ, Slekar KH, Strain J. 1995. A physiological role for *Saccharomyces cerevisiae* copper/zinc superoxide dismutase in copper buffering. J Biol Chem 270:29991–29997. https://doi.org/10.1074/jbc.270.50.29991.
3. Askwith C, Eide D, Van Ho A, Bernard PS, Li L, Davis-Kaplan S, Sipe DM, Kaplan J. 1994. The FET3 gene of *S. cerevisiae* encodes a multicopper oxidase required for ferrous iron uptake. Cell 76:403–410. https://doi.org/10.1016/0092-8674(94)90346-8.
4. Horn D, Barrientos A. 2008. Mitochondrial copper metabolism and delivery to cytochrome *c* oxidase. IUBMB Life 60:421–429. https://doi.org/10.1002/iub.50.
5. Dancis A, Haile D, Yuan DS, Klausner RD. 1994. The *Saccharomyces cerevisiae* copper transport protein (Ctr1p). Biochemical characterization, regulation by copper, and physiologic role in copper uptake. J Biol Chem 269:25660–25667.
6. Tamai KT, Gralla EB, Ellerby LM, Valentine JS, Thiele DJ. 1993. Yeast and mammalian metallothioneins functionally substitute for yeast copper-zinc superoxide dismutase. Proc Natl Acad Sci U S A 90:8013–8017. https://doi.org/10.1073/pnas.90.17.8013.
7. Wood LK, Thiele DJ. 2009. Transcriptional activation in yeast in response to copper deficiency involves copper-zinc superoxide dismutase. J Biol Chem 284:404–413. https://doi.org/10.1074/jbc.M807027200.
8. Jungmann J, Reins HA, Lee J, Romeo A, Hassett R, Kosman D, Jentsch S. 1993. MAC1, a nuclear regulatory protein related to Cu-dependent transcription factors is involved in Cu/Fe utilization and stress resistance in yeast. EMBO J 12:5051–5056. https://doi.org/10.1002/j.1460-2075.1993.tb06198.x.
9. Thiele DJ. 1988. ACE1 regulates expression of the *Saccharomyces cerevisiae* metallothionein gene. Mol Cell Biol 8:2745–2752. https://doi.org/10.1128/mcb.8.7.2745.
10. Welch J, Fogel S, Buchman C, Karin M. 1989. The CUP2 gene product regulates the expression of the CUP1 gene, coding for yeast metallothionein. EMBO J 8:255–260. https://doi.org/10.1002/j.1460-2075.1989.tb03371.x.
11. Serpe M, Joshi A, Kosman DJ. 1999. Structure-function analysis of the protein-binding domains of Mac1p, a copper-dependent transcriptional activator of copper uptake in *Saccharomyces cerevisiae*. J Biol Chem 274:29211–29219. https://doi.org/10.1074/jbc.274.41.29211.
12. Keller G, Bird A, Winge DR. 2005. Independent metalloregulation of Ace1 and Mac1 in *Saccharomyces cerevisiae*. Eukaryot Cell 4:1863–1871. https://doi.org/10.1128/EC.4.11.1863-1871.2005.
13. Ooi CE, Rabinovich E, Dancis A, Bonifacino JS, Klausner RD. 1996. Copper-dependent degradation of the *Saccharomyces cerevisiae* plasma membrane copper transporter Ctr1p in the apparent absence of endocytosis. EMBO J 15:3515–3523. https://doi.org/10.1002/j.1460-2075.1996.tb00720.x.
14. Liu J, Sitaram A, Burd CG. 2007. Regulation of copper-dependent endocytosis and vacuolar degradation of the yeast copper transporter, Ctr1p, by the Rsp5 ubiquitin ligase. Traffic 8:1375–1384. https://doi.org/10.1111/j.1600-0854.2007.00616.x.
15. Furst P, Hu S, Hackett R, Hamer D. 1988. Copper activates metallothionein gene transcription by altering the conformation of a specific DNA binding protein. Cell 55:705–717. https://doi.org/10.1016/0092-8674(88)90229-2.
16. Karpova TS, Kim MJ, Spriet C, Nalley K, Stasevich TJ, Kherrouche Z, Heliot L, McNally JG. 2008. Concurrent fast and slow cycling of a transcriptional activator at an endogenous promoter. Science 319:466–469. https://doi.org/10.1126/science.1150559.
17. Mehta GD, Ball DA, Eriksson PR, Chereji RV, Clark DJ, McNally JG, Karpova TS. 2018. Single-molecule analysis reveals linked cycles of RSC chromatin remodeling and Ace1p transcription factor binding in yeast. Mol Cell 72:875.e9–887.e9. https://doi.org/10.1016/j.molcel.2018.09.009.
18. Shen CH, Leblanc BP, Neal C, Akhavan R, Clark DJ. 2002. Targeted histone acetylation at the yeast CUP1 promoter requires the transcriptional activator, the TATA boxes, and the putative histone acetylase encoded by SPT10. Mol Cell Biol 22:6406–6416. https://doi.org/10.1128/mcb.22.18.6406-6416.2002.
19. Neuwald AF, Landsman D. 1997. GCN5-related histone N-acetyltransferases belong to a diverse superfamily that includes the yeast SPT10

protein. Trends Biochem Sci 22:154–155. https://doi.org/10.1016/s0968-0004(97)01034-7.
20. Kuo HC, Moore JD, Krebs JE. 2005. Histone H2A and Spt10 cooperate to regulate induction and autoregulation of the CUP1 metallothionein. J Biol Chem 280:104–111. https://doi.org/10.1074/jbc.M411437200.
21. Weiner A, Hsieh TH, Appleboim A, Chen HV, Rahat A, Amit I, Rando OJ, Friedman N. 2015. High-resolution chromatin dynamics during a yeast stress response. Mol Cell 58:371–386. https://doi.org/10.1016/j.molcel.2015.02.002.
22. Gasch AP, Spellman PT, Kao CM, Carmel-Harel O, Eisen MB, Storz G, Botstein D, Brown PO. 2000. Genomic expression programs in the response of yeast cells to environmental changes. Mol Biol Cell 11:4241–4257. https://doi.org/10.1091/mbc.11.12.4241.
23. Wang Z, Zang C, Rosenfeld JA, Schones DE, Barski A, Cuddapah S, Cui K, Roh TY, Peng W, Zhang MQ, Zhao K. 2008. Combinatorial patterns of histone acetylations and methylations in the human genome. Nat Genet 40:897–903. https://doi.org/10.1038/ng.154.
24. Barski A, Cuddapah S, Cui K, Roh TY, Schones DE, Wang Z, Wei G, Chepelev I, Zhao K. 2007. High-resolution profiling of histone methylations in the human genome. Cell 129:823–837. https://doi.org/10.1016/j.cell.2007.05.009.
25. Heintzman ND, Stuart RK, Hon G, Fu Y, Ching CW, Hawkins RD, Barrera LO, Van Calcar S, Qu C, Ching KA, Wang W, Weng Z, Green RD, Crawford GE, Ren B. 2007. Distinct and predictive chromatin signatures of transcriptional promoters and enhancers in the human genome. Nat Genet 39:311–318. https://doi.org/10.1038/ng1966.
26. Dai J, Hyland EM, Yuan DS, Huang H, Bader JS, Boeke JD. 2008. Probing nucleosome function: a highly versatile library of synthetic histone H3 and H4 mutants. Cell 134:1066–1078. https://doi.org/10.1016/j.cell.2008.07.019.
27. Morris SA, Rao B, Garcia BA, Hake SB, Diaz RL, Shabanowitz J, Hunt DF, Allis CD, Lieb JD, Strahl BD. 2007. Identification of histone H3 lysine 36 acetylation as a highly conserved histone modification. J Biol Chem 282:7632–7640. https://doi.org/10.1074/jbc.M607909200.
28. Mikkelsen TS, Ku M, Jaffe DB, Issac B, Lieberman E, Giannoukos G, Alvarez P, Brockman W, Kim T-K, Koche RP, Lee W, Mendenhall E, O'Donovan A, Presser A, Russ C, Xie X, Meissner A, Wernig M, Jaenisch R, Nusbaum C, Lander ES, Bernstein BE. 2007. Genome-wide maps of chromatin state in pluripotent and lineage-committed cells. Nature 448:553–560. https://doi.org/10.1038/nature06008.
29. Bernstein BE, Mikkelsen TS, Xie X, Kamal M, Huebert DJ, Cuff J, Fry B, Meissner A, Wernig M, Plath K, Jaenisch R, Wagschal A, Feil R, Schreiber SL, Lander ES. 2006. A bivalent chromatin structure marks key developmental genes in embryonic stem cells. Cell 125:315–326. https://doi.org/10.1016/j.cell.2006.02.041.
30. Butt TR, Sternberg EJ, Gorman JA, Clark P, Hamer D, Rosenberg M, Crooke ST. 1984. Copper metallothionein of yeast, structure of the gene, and regulation of expression. Proc Natl Acad Sci U S A 81:3332–3336. https://doi.org/10.1073/pnas.81.11.3332.
31. Karin M, Najarian R, Haslinger A, Valenzuela P, Welch J, Fogel S. 1984. Primary structure and transcription of an amplified genetic locus: the CUP1 locus of yeast. Proc Natl Acad Sci U S A 81:337–341. https://doi.org/10.1073/pnas.81.2.337.
32. Rojas JR, Trievel RC, Zhou J, Mo Y, Li X, Berger SL, Allis CD, Marmorstein R. 1999. Structure of tetrahymena GCN5 bound to coenzyme A and a histone H3 peptide. Nature 401:93–98. https://doi.org/10.1038/43487.
33. Wimalarathna RN, Pan PY, Shen CH. 2012. Chromatin repositioning activity and transcription machinery are both recruited by Ace1p in yeast CUP1 activation. Biochem Biophys Res Commun 422:658–663. https://doi.org/10.1016/j.bbrc.2012.05.047.
34. Smolle M, Venkatesh S, Gogol MM, Li H, Zhang Y, Florens L, Washburn MP, Workman JL. 2012. Chromatin remodelers Isw1 and Chd1 maintain chromatin structure during transcription by preventing histone exchange. Nat Struct Mol Biol 19:884–892. https://doi.org/10.1038/nsmb.2312.
35. Venkatesh S, Smolle M, Li H, Gogol MM, Saint M, Kumar S, Natarajan K, Workman JL. 2012. Set2 methylation of histone H3 lysine 36 suppresses histone exchange on transcribed genes. Nature 489:452–455. https://doi.org/10.1038/nature11326.
36. Sen P, Dang W, Donahue G, Dai J, Dorsey J, Cao X, Liu W, Cao K, Perry R, Lee JY, Wasko BM, Carr DT, He C, Robison B, Wagner J, Gregory BD, Kaeberlein M, Kennedy BK, Boeke JD, Berger SL. 2015. H3K36 methylation promotes longevity by enhancing transcriptional fidelity. Genes Dev 29:1362–1376. https://doi.org/10.1101/gad.263707.115.
37. Millar CB, Grunstein M. 2006. Genome-wide patterns of histone modifications in yeast. Nat Rev Mol Cell Biol 7:657–666. https://doi.org/10.1038/nrm1986.
38. Grant PA, Duggan L, Cote J, Roberts SM, Brownell JE, Candau R, Ohba R, Owen-Hughes T, Allis CD, Winston F, Berger SL, Workman JL. 1997. Yeast Gcn5 functions in two multisubunit complexes to acetylate nucleosomal histones: characterization of an Ada complex and the SAGA (Spt/Ada) complex. Genes Dev 11:1640–1650. https://doi.org/10.1101/gad.11.13.1640.
39. Vermeulen M, Mulder KW, Denissov S, Pijnappel WW, van Schaik FM, Varier RA, Baltissen MP, Stunnenberg HG, Mann M, Timmers HT. 2007. Selective anchoring of TFIID to nucleosomes by trimethylation of histone H3 lysine 4. Cell 131:58–69. https://doi.org/10.1016/j.cell.2007.08.016.
40. Fillingham J, Recht J, Silva AC, Suter B, Emili A, Stagljar I, Krogan NJ, Allis CD, Keogh MC, Greenblatt JF. 2008. Chaperone control of the activity and specificity of the histone H3 acetyltransferase Rtt109. Mol Cell Biol 28:4342–4353. https://doi.org/10.1128/MCB.00182-08.
41. Krebs JE, Fry CJ, Samuels ML, Peterson CL. 2000. Global role for chromatin remodeling enzymes in mitotic gene expression. Cell 102:587–598. https://doi.org/10.1016/s0092-8674(00)00081-7.
42. Boyd SD, Calvo JS, Liu L, Ullrich MS, Skopp A, Meloni G, Winkler DD. 2019. The yeast copper chaperone for copper-zinc superoxide dismutase (CCS1) is a multifunctional chaperone promoting all levels of SOD1 maturation. J Biol Chem 294:1956–1966. https://doi.org/10.1074/jbc.RA118.005283.
43. Culotta VC, Howard WR, Liu XF. 1994. CRS5 encodes a metallothionein-like protein in *Saccharomyces cerevisiae*. J Biol Chem 269:25295–25302.
44. Jensen LT, Howard WR, Strain JJ, Winge DR, Culotta VC. 1996. Enhanced effectiveness of copper ion buffering by CUP1 metallothionein compared with CRS5 metallothionein in *Saccharomyces cerevisiae*. J Biol Chem 271:18514–18519. https://doi.org/10.1074/jbc.271.31.18514.
45. Jacobson T, Navarrete C, Sharma SK, Sideri TC, Ibstedt S, Priya S, Grant CM, Christen P, Goloubinoff P, Tamas MJ. 2012. Arsenite interferes with protein folding and triggers formation of protein aggregates in yeast. J Cell Sci 125:5073–5083. https://doi.org/10.1242/jcs.107029.
46. Jacobson T, Priya S, Sharma SK, Andersson S, Jakobsson S, Tanghe R, Ashouri A, Rauch S, Goloubinoff P, Christen P, Tamas MJ. 2017. Cadmium causes misfolding and aggregation of cytosolic proteins in yeast. Mol Cell Biol 37:e00490-16. https://doi.org/10.1128/MCB.00490-16.
47. Sahu RK, Saha N, Das L, Sahu PK, Sariki SK, Tomar RS. 2020. SWI/SNF chromatin remodelling complex contributes to clearance of cytoplasmic protein aggregates and regulates unfolded protein response in *Saccharomyces cerevisiae*. FEBS J 287:3024–3041. https://doi.org/10.1111/febs.15180.
48. Arnesano F, Scintilla S, Calo V, Bonfrate E, Ingrosso C, Losacco M, Pellegrino T, Rizzarelli E, Natile G. 2009. Copper-triggered aggregation of ubiquitin. PLoS One 4:e7052. https://doi.org/10.1371/journal.pone.0007052.
49. Rasia RM, Bertoncini CW, Marsh D, Hoyer W, Cherny D, Zweckstetter M, Griesinger C, Jovin TM, Fernandez CO. 2005. Structural characterization of copper(II) binding to alpha-synuclein: insights into the bioinorganic chemistry of Parkinson's disease. Proc Natl Acad Sci U S A 102:4294–4299. https://doi.org/10.1073/pnas.0407881102.
50. Malinovska L, Kroschwald S, Munder MC, Richter D, Alberti S. 2012. Molecular chaperones and stress-inducible protein-sorting factors coordinate the spatiotemporal distribution of protein aggregates. Mol Biol Cell 23:3041–3056. https://doi.org/10.1091/mbc.E12-03-0194.
51. Choe YJ, Park SH, Hassemer T, Korner R, Vincenz-Donnelly L, Hayer-Hartl M, Hartl FU. 2016. Failure of RQC machinery causes protein aggregation and proteotoxic stress. Nature 531:191–195. https://doi.org/10.1038/nature16973.
52. Park SH, Kukushkin Y, Gupta R, Chen T, Konagai A, Hipp MS, Hayer-Hartl M, Hartl FU. 2013. PolyQ proteins interfere with nuclear degradation of cytosolic proteins by sequestering the Sis1p chaperone. Cell 154:134–145. https://doi.org/10.1016/j.cell.2013.06.003.
53. Shen CH, Leblanc BP, Alfieri JA, Clark DJ. 2001. Remodeling of yeast CUP1 chromatin involves activator-dependent repositioning of nucleosomes over the entire gene and flanking sequences. Mol Cell Biol 21:534–547. https://doi.org/10.1128/MCB.21.2.534-547.2001.
54. Loffreda A, Jacchetti E, Antunes S, Rainone P, Daniele T, Morisaki T, Bianchi ME, Tacchetti C, Mazza D. 2017. Live-cell p53 single-molecule binding is modulated by C-terminal acetylation and correlates with transcriptional activity. Nat Commun 8:313. https://doi.org/10.1038/s41467-017-00398-7.
55. Morisaki T, Muller WG, Golob N, Mazza D, McNally JG. 2014. Single-molecule analysis of transcription factor binding at transcription sites in live cells. Nat Commun 5:4456. https://doi.org/10.1038/ncomms5456.
56. Paakinaho V, Presman DM, Ball DA, Johnson TA, Schiltz RL, Levitt P, Mazza

D, Morisaki T, Karpova TS, Hager GL. 2017. Single-molecule analysis of steroid receptor and cofactor action in living cells. Nat Commun 8:15896. https://doi.org/10.1038/ncomms15896.
57. Poorey K, Viswanathan R, Carver MN, Karpova TS, Cirimotich SM, McNally JG, Bekiranov S, Auble DT. 2013. Measuring chromatin interaction dynamics on the second time scale at single-copy genes. Science 342:369–372. https://doi.org/10.1126/science.1242369.
58. Li XY, Virbasius A, Zhu X, Green MR. 1999. Enhancement of TBP binding by activators and general transcription factors. Nature 399:605–609. https://doi.org/10.1038/21232.
59. Krogan NJ, Kim M, Tong A, Golshani A, Cagney G, Canadien V, Richards DP, Beattie BK, Emili A, Boone C, Shilatifard A, Buratowski S, Greenblatt J. 2003. Methylation of histone H3 by Set2 in *Saccharomyces cerevisiae* is linked to transcriptional elongation by RNA polymerase II. Mol Cell Biol 23:4207–4218. https://doi.org/10.1128/mcb.23.12.4207-4218.2003.
60. Xiao T, Hall H, Kizer KO, Shibata Y, Hall MC, Borchers CH, Strahl BD. 2003. Phosphorylation of RNA polymerase II CTD regulates H3 methylation in yeast. Genes Dev 17:654–663. https://doi.org/10.1101/gad.1055503.
61. Bannister AJ, Schneider R, Myers FA, Thorne AW, Crane-Robinson C, Kouzarides T. 2005. Spatial distribution of di- and tri-methyl lysine 36 of histone H3 at active genes. J Biol Chem 280:17732–17736. https://doi.org/10.1074/jbc.M500796200.
62. Edmunds JW, Mahadevan LC, Clayton AL. 2008. Dynamic histone H3 methylation during gene induction: HYPB/Setd2 mediates all H3K36 trimethylation. EMBO J 27:406–420. https://doi.org/10.1038/sj.emboj.7601967.
63. Teissandier A, Bourc'his D. 2017. Gene body DNA methylation conspires with H3K36me3 to preclude aberrant transcription. EMBO J 36:1471–1473. https://doi.org/10.15252/embj.201796812.
64. DiFiore JV, Ptacek TS, Wang Y, Li B, Simon JM, Strahl BD. 2020. Unique and shared roles for histone H3K36 methylation states in transcription regulation functions. Cell Rep 31:107751. https://doi.org/10.1016/j.celrep.2020.107751.
65. Chung RS, Howells C, Eaton ED, Shabala L, Zovo K, Palumaa P, Sillard R, Woodhouse A, Bennett WR, Ray S, Vickers JC, West AK. 2010. The native copper- and zinc-binding protein metallothionein blocks copper-mediated Abeta aggregation and toxicity in rat cortical neurons. PLoS One 5:e12030. https://doi.org/10.1371/journal.pone.0012030.
66. Okita Y, Rcom-H'cheo-Gauthier AN, Goulding M, Chung RS, Faller P, Pountney DL. 2017. Metallothionein, copper and alpha-synuclein in alpha-synucleinopathies. Front Neurosci 11:114. https://doi.org/10.3389/fnins.2017.00114.
67. Paik SR, Shin HJ, Lee JH, Chang CS, Kim J. 1999. Copper(II)-induced self-oligomerization of alpha-synuclein. Biochem J 340:821–828. https://doi.org/10.1042/bj3400821.
68. Attar N, Campos OA, Vogelauer M, Cheng C, Xue Y, Schmollinger S, Salwinski L, Mallipeddi NV, Boone BA, Yen L, Yang S, Zikovich S, Dardine J, Carey MF, Merchant SS, Kurdistani SK. 2020. The histone H3-H4 tetramer is a copper reductase enzyme. Science 369:59–64. https://doi.org/10.1126/science.aba8740.
69. Longtine MS, McKenzie A, III, Demarini DJ, Shah NG, Wach A, Brachat A, Philippsen P, Pringle JR. 1998. Additional modules for versatile and economical PCR-based gene deletion and modification in *Saccharomyces cerevisiae*. Yeast 14:953–961. https://doi.org/10.1002/(SICI)1097-0061(199807)14:10<953::AID-YEA293>3.0.CO;2-U.
70. O'Driscoll J, Clare D, Saibil H. 2015. Prion aggregate structure in yeast cells is determined by the Hsp104-Hsp110 disaggregase machinery. J Cell Biol 211:145–158. https://doi.org/10.1083/jcb.201505104.
71. Schmitt ME, Brown TA, Trumpower BL. 1990. A rapid and simple method for preparation of RNA from *Saccharomyces cerevisiae*. Nucleic Acids Res 18:3091–3092. https://doi.org/10.1093/nar/18.10.3091.
72. Szymanski EP, Kerscher O. 2013. Budding yeast protein extraction and purification for the study of function, interactions, and post-translational modifications. J Vis Exp 2013:e50921. https://doi.org/10.3791/50921.
73. Shirra MK, Rogers SE, Alexander DE, Arndt KM. 2005. The Snf1 protein kinase and Sit4 protein phosphatase have opposing functions in regulating TATA-binding protein association with the *Saccharomyces cerevisiae* INO1 promoter. Genetics 169:1957–1972. https://doi.org/10.1534/genetics.104.038075.